205

SATELLITE & MESOMETEOROLOGY
RESEARCH PROJECT

Department of the Geophysical Sciences
The University of Chicago

ANDREWS AFB MICROBURST

by

Tetsuya Theodore Fujita

SMRP Research Paper 205

Paper presented at Andrews AFB on Dec. 5, 1983

Acknowledgements

The author wishes to express his sincere appreciation to Lt. Col. William Kiser of the Andrews AFB Weather Station and Lt. Col. George Duffield of the Air Weather Service, Scott Air Force Base for their assistance in obtaining the weather and damage information in and around the Air Force Base.

The research work presented in this paper has been sponsored by three government agencies: National Science Foundation under Grant No. ATM8109828, National Aeronautics and Space Administration under Grant No. NGR-14-001-008, and National Environmental Satellite, Data, and Information Service under Grant No. NA80AAD00001.

SMRP Research Paper 205

Satellite & Mesometeorology Research Project

Department of the Geophysical Sciences
The University of Chicago

ANDREWS AFB MICROBURST

by

Tetsuya Theodore Fujita
Professor of Meteorology

The University of Chicago
Chicago, Illinois 60637

■ Paper presented at Andrews Air Force Base on December 5, 1983

PREFACE

Late in the 1970s, the author's concept of the "downburst" (a strong downdraft which induces an outburst of damaging winds on or near the ground), originated after the analysis of the JFK accident on June 24, 1975, was regarded as controversial. At that time, only a handful of meteorologists could visualize a downdraft descending as low as 100m (300 ft) above the ground before spreading out violently. On the contrary, the downdraft, as revealed by the Thunderstorm Project (1946 - 47), was assumed to lose its downflow speed long before reaching the ground. Consequently, an aircraft flying beneath a downdraft would not be affected by either downflow or strong outflow winds as long as its flight altitude remained less than, say 100m (300 ft) above the ground.

NIMROD Project in 1978 was operated by Fujita and Srivastava of the University of Chicago as co-investigators. Three Doppler radars and 27 automated surface stations were used. 50 microbursts were confirmed by the surface station data. One of the Doppler radars recorded a peak outflow speed of 62 kts located only 100 to 150 feet above the ground.

JAWS Project in 1982 was operated jointly by the University of Chicago and the National Center for Atmospheric Research, with Fujita (U of C) and McCarthy and Wilson (NCAR) as co-investigators. The purpose of this project was to determine the scale, life, and structure of downbursts. Of the numerous downburst winds recorded by 27 surface automated stations, 186 were less than 2 nautical miles in size, being classified as planetary MISOSCALE (40 to 4000 meter or 130 to 13,120 ft) disturbances.

Based on NIMROD (Northern Illinois Meteorological Research on Downburst) and JAWS (Joint Airport Weather Studies) researches, the author now subclassifies the "downburst" into "macroburst" and "microburst".

- MACROBURST - A large (mesoscale) sized downburst. An intense macroburst often causes widespread, tornado-like damage. Damaging winds, lasting 5 to 20 minutes, could reach as much as 150 mph.

- MICROBURST - A small (misoscale) sized downburst with peak winds, lasting only 2 to 5 minutes, which could reach as much as 150 mph. A microburst induces dangerous tailwind and downflow shear which cannot always be detected by ground-based anemometers.

The 149+ mph peak wind recorded at Andrews AFB, six minutes after the touchdown of Air Force One, turned out to be the strongest microburst wind ever documented. The purpose of this paper is to clarify the nature of the Andrews AFB microburst, leading to a possible method of detecting microburst winds before they reach the ground.

Tetsuya Theodore Fujita

November 17, 1983

TABLE OF CONTENTS

1. TIME OF ANDREWS AIR FORCE BASE MICROBURST

Early in the afternoon of August 1, 1983, a very strong microburst swept across the runway area of Andrews Air Force Base. Fortunately, Air Force One with the President on board landed at 1404 on the dry runway before the onset of the microburst winds. It was a close call, however.

Special observations taken between 1405 and 1427 EDT presented in Table 1 reveals that a 50 kt gust was in progress at 1410 EDT. The correction of the gust speeds in the table was made at a later time on the basis of the wind trace which had recorded the 130+ kts wind speed. Winds were measured by GMQ-20, a propeller anemometer (16ft tall) located near the north end of the runway.

In determining the accurate peak-gust time, it was assumed that the weather observer wrote the time, 1410 EDT (1810 GMT), when winds were gusting to 50 kts. On the other hand, the time of the first 50 kt gust on the wind trace was 1413 EDT, which is 3 minutes slower than the observer's time. The 3 minute correction of the wind-trace time results in a good agreement between the 14 kt gust observed at 1419 EDT and the two 14 kt gusts recorded approximately at 1419 EDT.

The red time lines superimposed on wind and pressure traces denote the most probable times of these events.

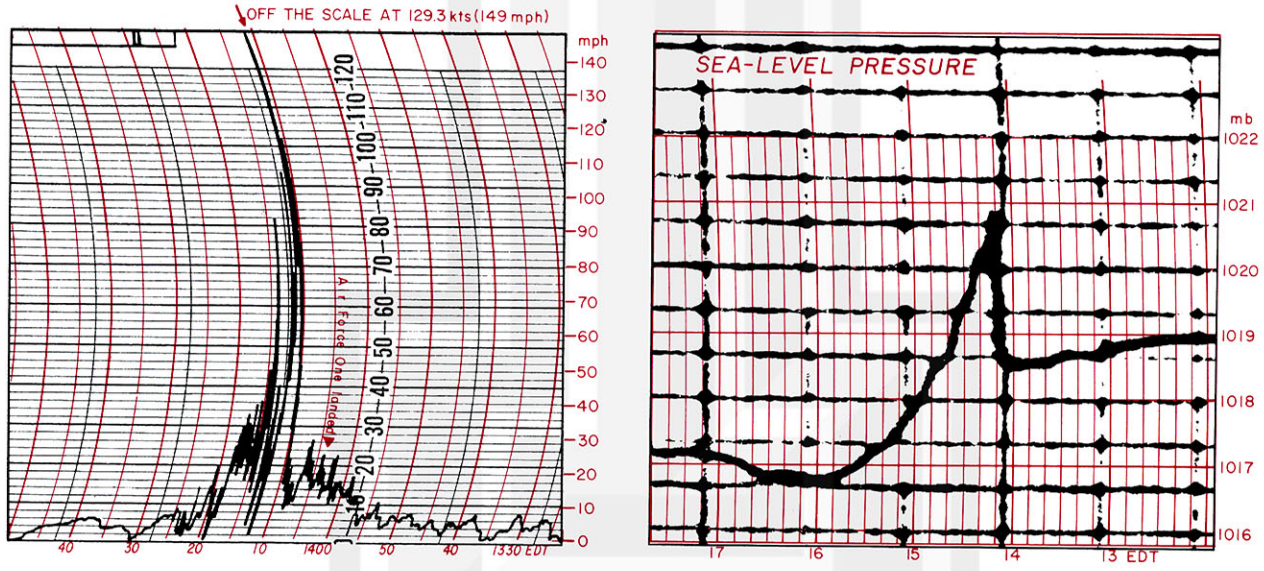

Fig. 1. Wind (left) and pressure (right) traces of the Andrews Air Force Base microburst on August 1, 1983. Curved lines superimposed in red denote the most probable time of the wind and pressure events. Note that the wind chart time was advanced by three minutes and the barograph time was delayed by five minutes.

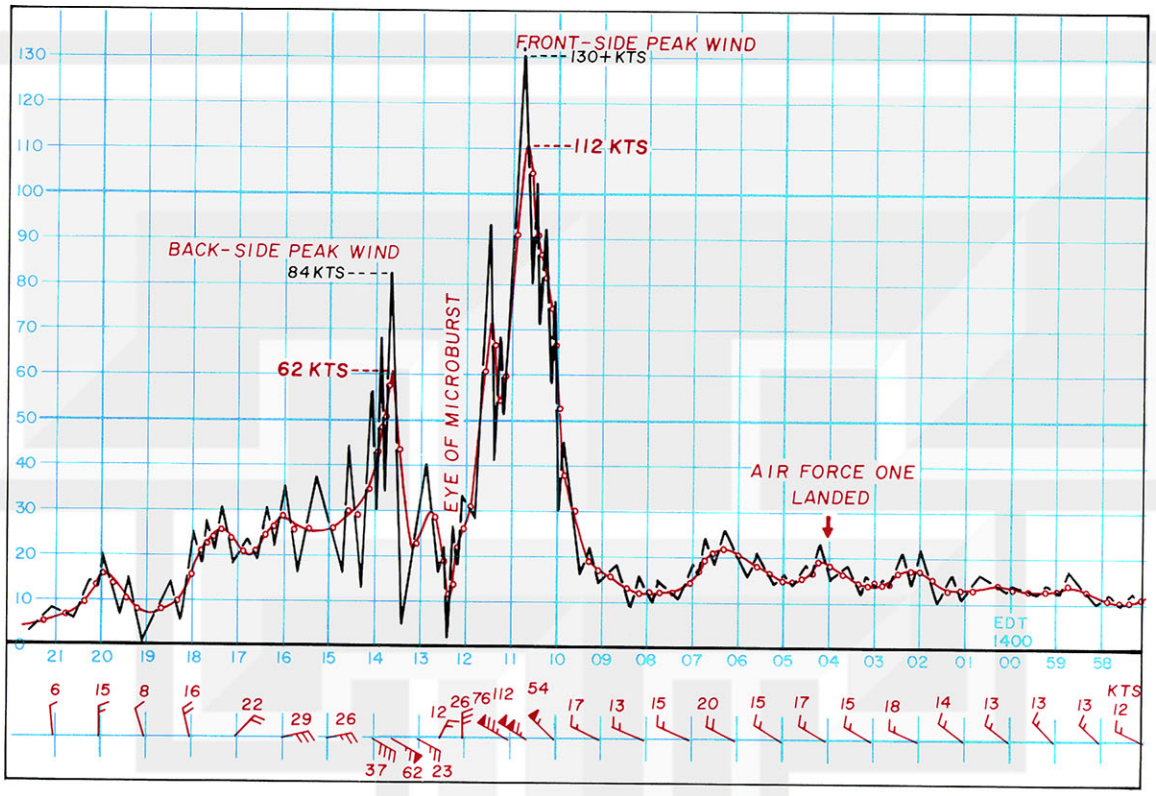

Fig. 2. Gusts and lulls of the microburst winds plotted by determining these wind speeds on an enlarged wind trace. Red circles denote the mean wind speeds of the successive gust, lull, gust, lull,.....speeds. Vector winds of the mean speeds are plotted with the standard meteorological symbols.

Table 1. Special observations taken at Andrews AFB before, during, and after the microburst on August 1, 1983.

Time (EDT)	1405	1407	1410	1419	1427
Wind direction	300°	280°	E300°	340°	90°
Wind speed	14	18	10	7	6 kts
Gust	G23	G27	G50	G14	-
Corrected gust	-	-	G130	G33	-
Thunder	yes	yes	yes	yes	yes
Rain	no	RW-	RW+	RW-	RW-
1/4" Hail	no	no	began	ended	no

2. WIND DAMAGE IN AND AROUND THE AIR FORCE BASE

According to the helicopter survey performed by the Air Weather Service on August 2, there were numerous wind damages in and around the Base. As shown in Fig. 3, the anemometer near the north end of two parallel runways measured a 130+ kts gust from the west-northwest at 1410 EDT. Four minutes later, at 1414 EDT, the same anemometer measured a 82 kts gust which came from the opposite direction (from east-southeast). This reversal of the wind direction, along with the "calm" occurring between these two peak gusts, implies the passage of the microburst center just to the north of the anemometer. The dead center of the microburst missed the anemometer by only 0.1 mile.

The direction of damaging winds varied considerably within the base. Buildings S-3416 and S-3417 located on the east side of the base were damaged by strong west to northwest winds (see Fig. 4). Trees in the northeast section of the base were uprooted by the west winds. The Arts and Craft Center, 0.3 mile to the west of the Base Weather Station, was damaged by north-northeast winds. These damaging winds diverged out from the northern part of the base. It is very likely that the microburst first hit the ground approximately 1 mile to the northwest of the anemometer. Then its wind field expanded rapidly across the runway area.

An eyewitness account of D. Robert Munro from his Forestville home, 2 miles north of the approach end of runway 19, while the Base was experiencing strong microburst winds, is striking. Shortly after seeing Air Force One land on runway 19R, he saw a shower to the south of his home, directly over the base area. The wind at his location was variable with a few gusts only up to 5 to 6 kts. In other words, it was practically calm when the Andrews anemometer, 2.3 miles south of his home, recorded the 130+ kts gust. The horizontal extent of the microburst was very small.

However, the broken tree branches reported from the Filippelli site near the southwest corner of the map in Fig. 3 may have been caused by an entirely separate microburst, because several microbursts often occur in close proximity to each other. A brief report of the storm at his site reads " Heavy thunderstorm approximately at 1400 EDT with strong winds, rain, and pea sized hail. Many tree branches broken. Total rainfall 0.73 inch".

1/4" or pea sized hail was reported from the three sites in Fig. 3. They are Filippelli, Andrews Base Weather Station, and Paroczay, just to the north of Capital Beltway. These reports by no means rule out the occurrence of similar hail at other locations. It is likely that most of the storm areas experienced hail.

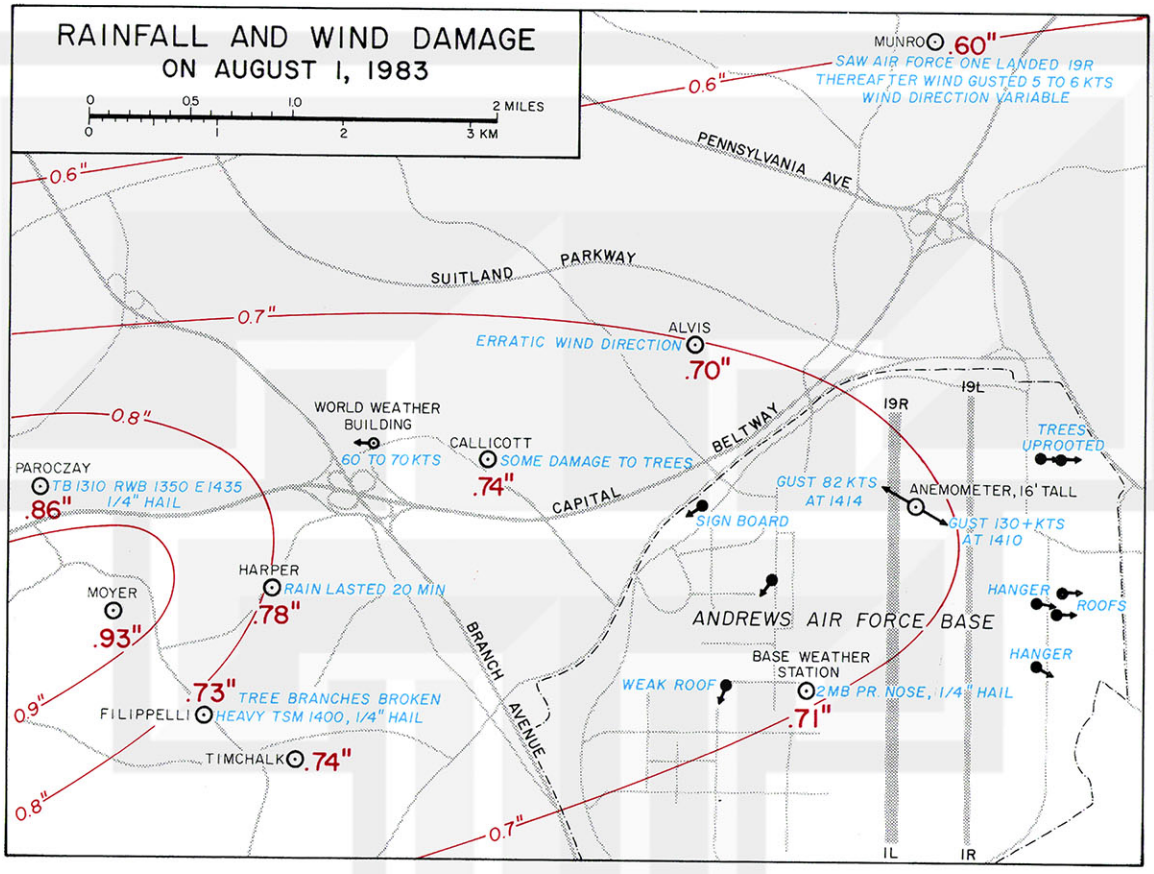

Fig. 3. Distribution of rainfall and wind damage in and around Andrews AFB caused by the microburst storm on August 1, 1983. Damaging winds are shown by black circles with arrows attached. Rainfalls are in 0.01" unit.

0.93", the largest rainfall amount inside the map, was measured at the Moyer site near the southwest corner of Fig. 3. Rainfall amounts decreased gradually toward the east, suggesting that the parent thunderstorm over the Andrews AFB area was in its post-mature stage.

Apparently, Capital Beltway was not affected by an excessive crosswind which could cause traffic accidents. The lack of storm-related accidents on the Beltway suggests that the microburst descended to the ground near the Beltway northwest of the Andrews anemometer.

The Alvis site, 0.5 mile northwest of the Beltway, reported erratic wind direction during the storm. The report implies that the fury of the microburst was not experienced at this site.

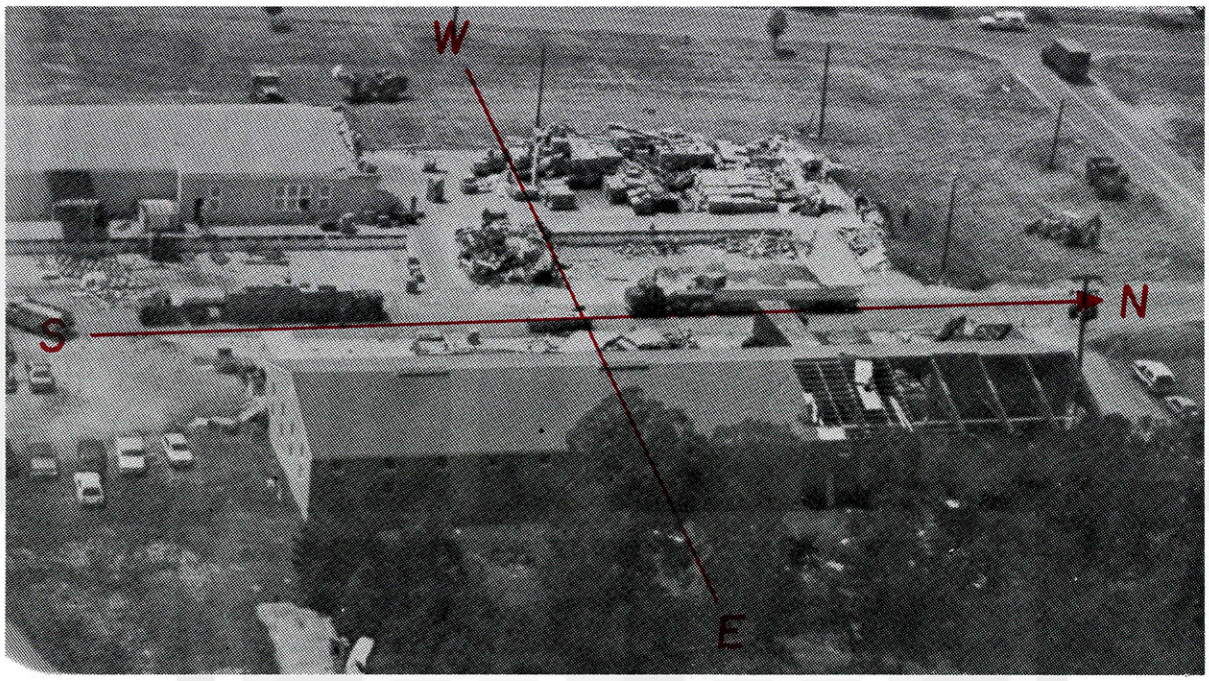

Fig. 4. Building S-3416 (background) was damaged by westerly winds and the structure has been cleaned up. Roof of S-3417 blew off toward east. Limbs were broken off and some trees were uprooted in this area. (USAF photo)

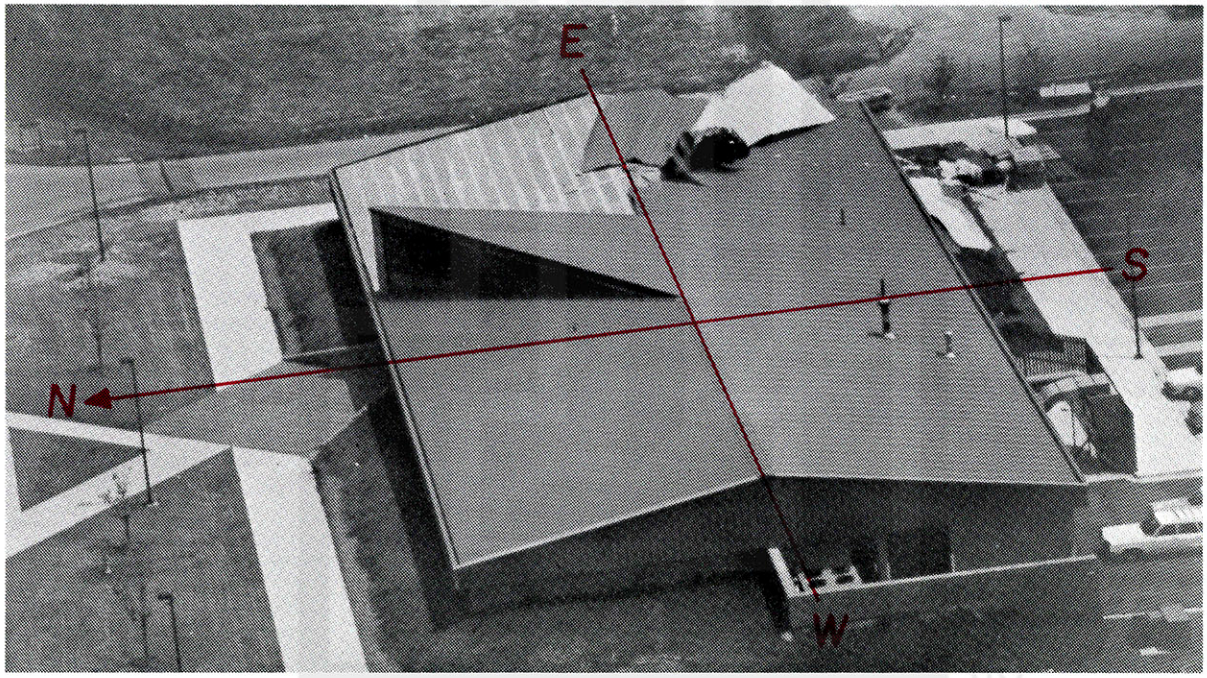

Fig. 5. The roof of the Arts and Craft Center in the Air Force Base damaged by the wind. Photo is looking toward the east-southeast. The direction of the damaging wind was north-northeast (USAF photo).

3. PARENT ECHO FROM PATUXENT RIVER RADAR

A sequence in Figs. 6 and 7 shows the Patuxent River radar photos selected at approximately 15-minute intervals. The parent cloud at 1233 was a small echo 64 n.m. to the west-southwest of Andrews AFB, which is located 38 n.m. northwest of the radar.

Another small echo (outlined with dashed red line) moved eastward at high speed, contacting the parent echo at 1301 EDT. Thereafter, these two small echoes merged into one larger echo and the intensity level increased from Level 4 to 5.

At 1415 EDT, a few minutes after the microburst at the Base, the downwind section of the parent echo began drifting northeast. By 1430, the echo had bulged out. Photos at 1445 and 1500 show that the bulge, consisting probably of falling particles from an anvil, drifted away from the core region of the parent cell.

Radar observations summarized in Table 2 indicate that the echo-top height remained at 42,000 ft for over one hour. It is of interest to find that the observed echo top did not pass over Andrews AFB; instead it was located 3 n.m. to the northwest of the Base while the microburst winds were in progress (refer to Andrews AFB coordinates of the parent echo).

Three radar photos in Fig. 8 also confirm the relative location between the echo and the AFB. The top photo at 1405 EDT taken with 10° elevation shows the parent echo at the AGL height,

$$41 \text{ n.m.} \times \sin 10° = 13.2 \text{ km} = 43{,}000 \text{ ft}$$

which is higher than the measured echo-top. Such a difference is usually due to beam width and possible side-lobe effects.

Table 2. Parent cloud of Andrews AFB microburst observed by the Patuxent River radar. Andrews on the Patuxent coordinates is 326° at 38 n.m. ADW---Andrews, NHK---Patuxent River

Time *EDT*	ADW coordinates *Azimuth Range*	NHK coordinates *Azimuth Range*	Dia. *n.m.*	Dir. *deg*	Spd. *kts*	Echo top *feet*	Level
1233	253° 64 nm	288° 64 nm	6	-	-	-	-
1303	258 28	298 55	9	-	-	42,000	4
1325	261 19	306 49	10	250	28	42,000	5
1401	285 05	322 42	8	250	22	42,000	5
1410	E332 E03	E327 E41	E10	E250	E21	E42,000	E5
1425	041 06	334 40	12	250	20	42,000	6

E -- interpolation between 1401 and 1425 EDT data

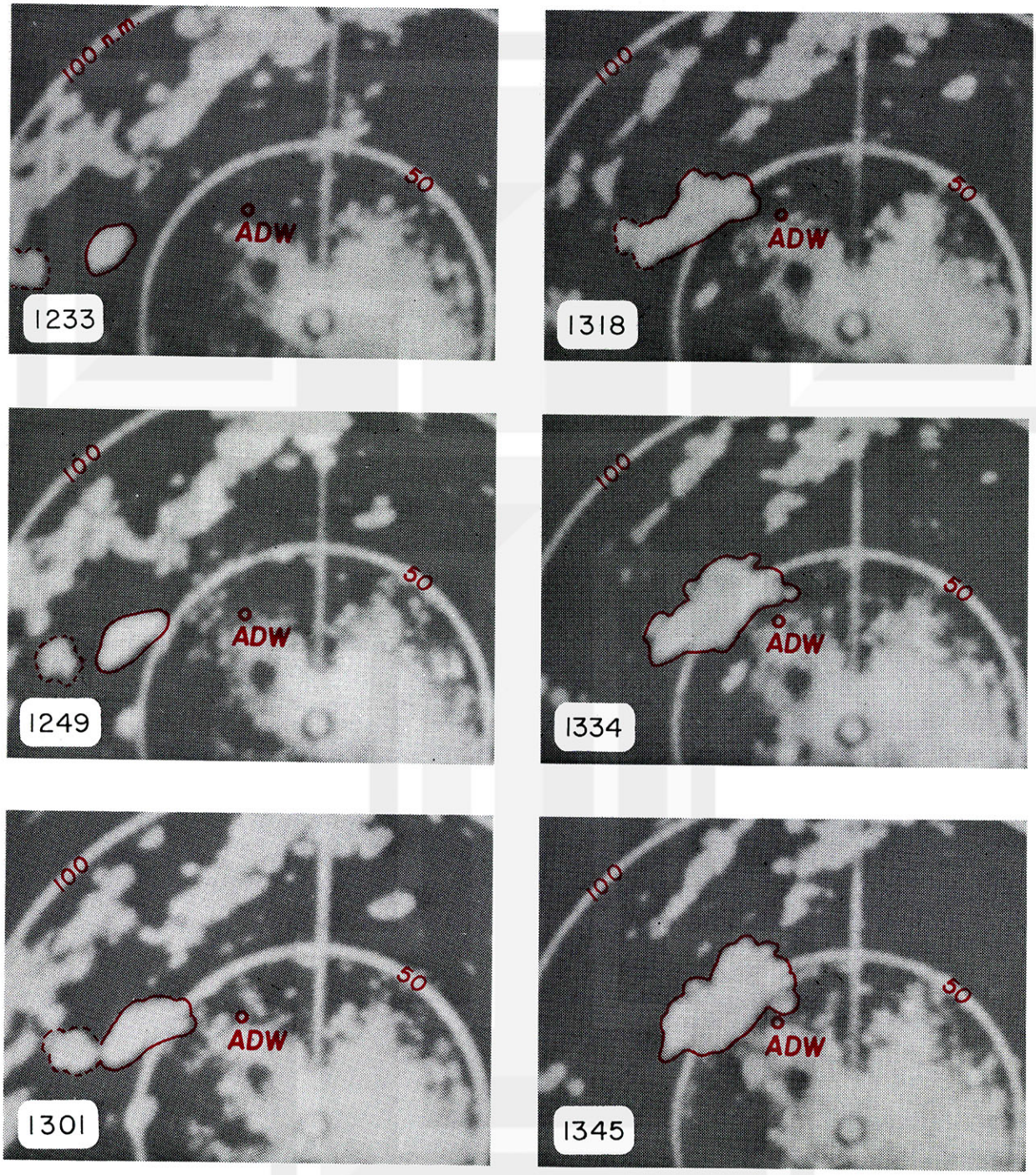

Fig. 6. Parent radar echoes (red outlines) of the microburst depicted by the Patuxent River radar. Pictures were selected approximately at 15-min. intervals between 1233 and 1345 EDT August 1, 1983.

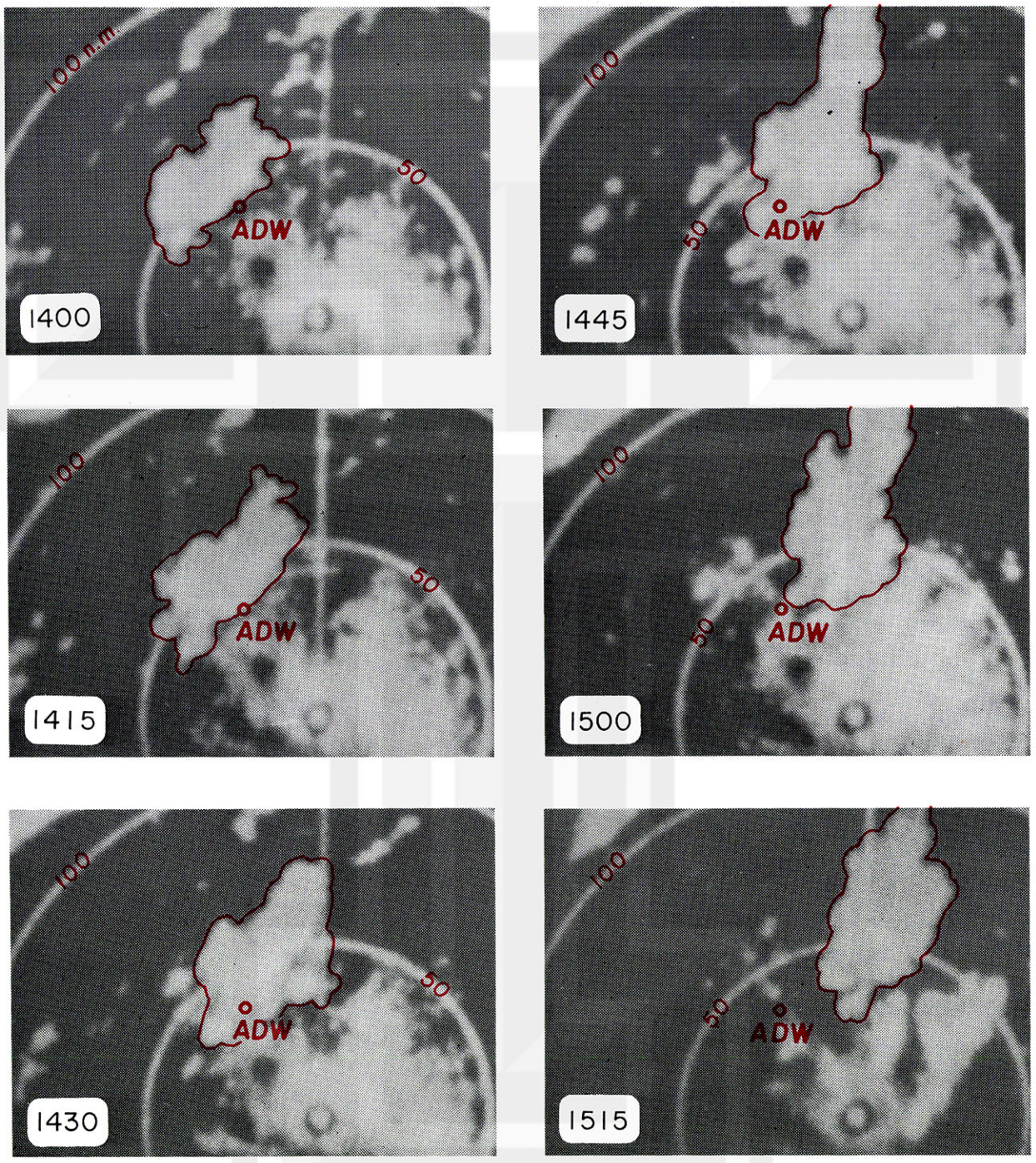

Fig. 7. Parent radar echoes (red outlines) of the microburst depicted by the Patuxent River radar. Pictures were selected approximately at 15-min. intervals between 1400 and 1515 EDT August 1, 1983.

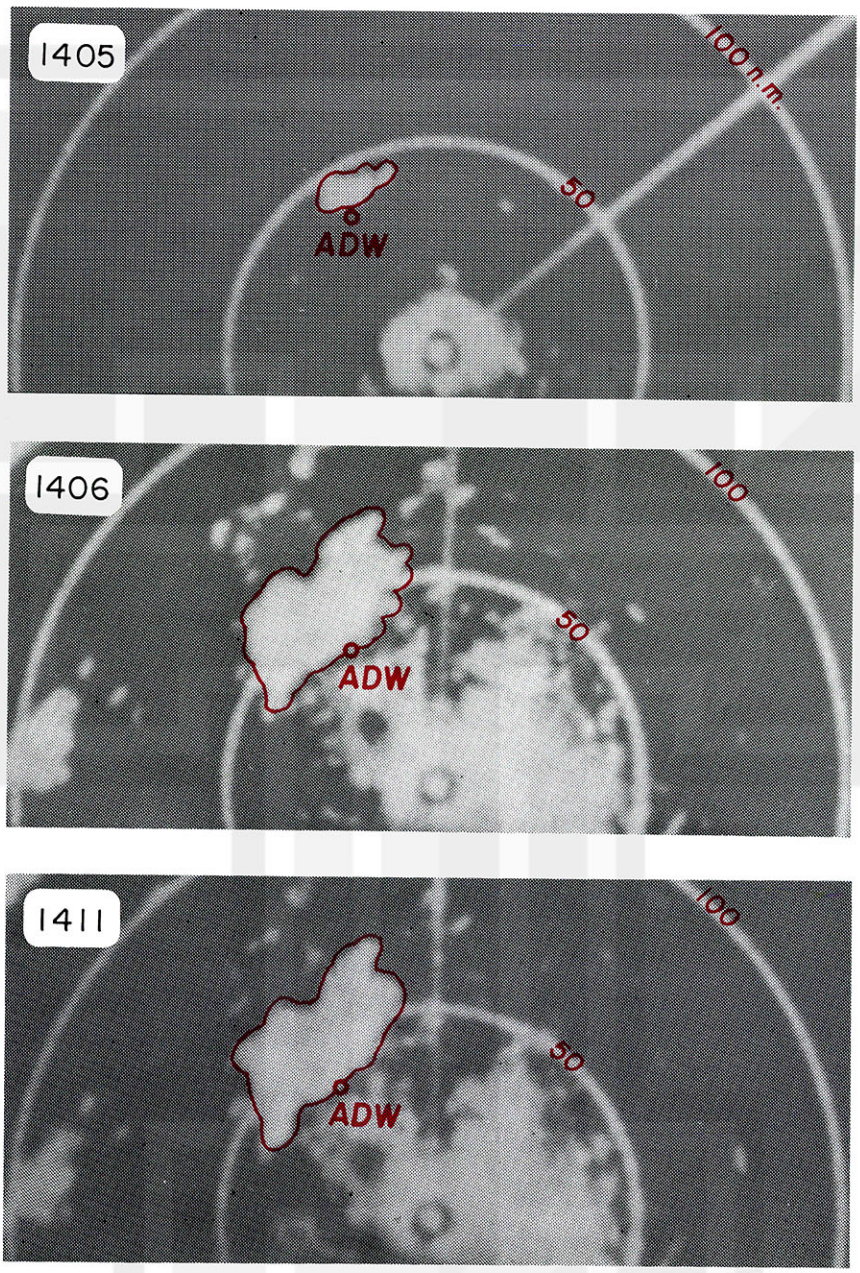

Fig. 8. Parent radar echo (red outlines) within one to two minutes of Air Force One landing. Upper photo scanned with 10° elevation and lower photo with 1°. Photo at the bottom shows the parent echo at the time of the highest gust in excess of 130 kts. Andrews AFB was located on the south edge of the parent echo. The microburst, apparently, dashed out of the echo toward the east-southeast.

Radar observations at Patuxent River at 1401 EDT indicate that the echo top at 42,000' was moving 250° at 20 kts. Echo intensity level 5, TRW X, D 8 mi.

At 1406 EDT, two minutes after the touchdown of Air Force One, Andrews AFB was located on the southeast edge of the parent echo scanned with near zero elevation angle. During the microburst time as well, the AFB was on the southeast edge of the low-elevation echo, strongly suggesting that the microburst downflow shot out of the parent echo toward the east-southeast.

The slant angle connecting the reported echo top at 42,000 ft (7 n.m.) with the microburst location, approximately 3 n.m. to the southeast, is 23°. This means that the nadir angle of the microburst on the ground as viewed from the echo top was 23° from the nadir (see a diagram below).

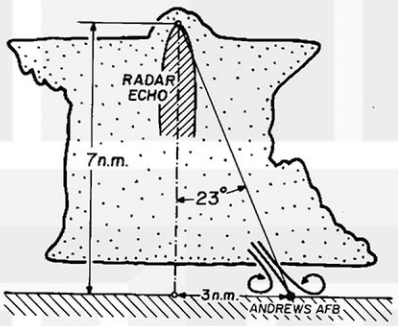

4. CLOUD TOP TEMPERATURE FROM GOES EAST SATELLITE

GOES East geostationary satellite took measurements of both infrared (IR) and visible radiation from the parent cloud of the Andrews AFB microburst. Since nobody suspected the occurrence of the 130+ kts wind, satellite pictures were taken for every 30 minutes, which is the normal interval for non-severe weather situations.

Fig. 9 presents a sequence of GOES East imagery. 1230, 1430, and 1530 EDT pictures show visible imagery only, while 1300, 1400, 1500, and 1600 EDT pictures show visible imagery combined with the field of IR temperature. The outer black boundaries denote -34°C and inner black boundaries, -60°C.

No indication of the parent cloud is evidenced at 1200 EDT. However, a towering cumulus elongated in the WSW-ENE direction is seen to the south-southwest of Washington, D.C. at 1230 EDT. The location of the Andrews cloud, A, and another storm, P, formed near the Patuxent radar station, are identified with red dots on the satellite pictures. The Andrews cloud was neither the largest nor the coldest cloud in the area. One could find numerous other storm clouds which appear far worse than the Andrews cloud. As a rule, unexpected microbursts are induced by innocuous clouds. This unfortunate fact makes microburst watches more difficult than tornado watches.

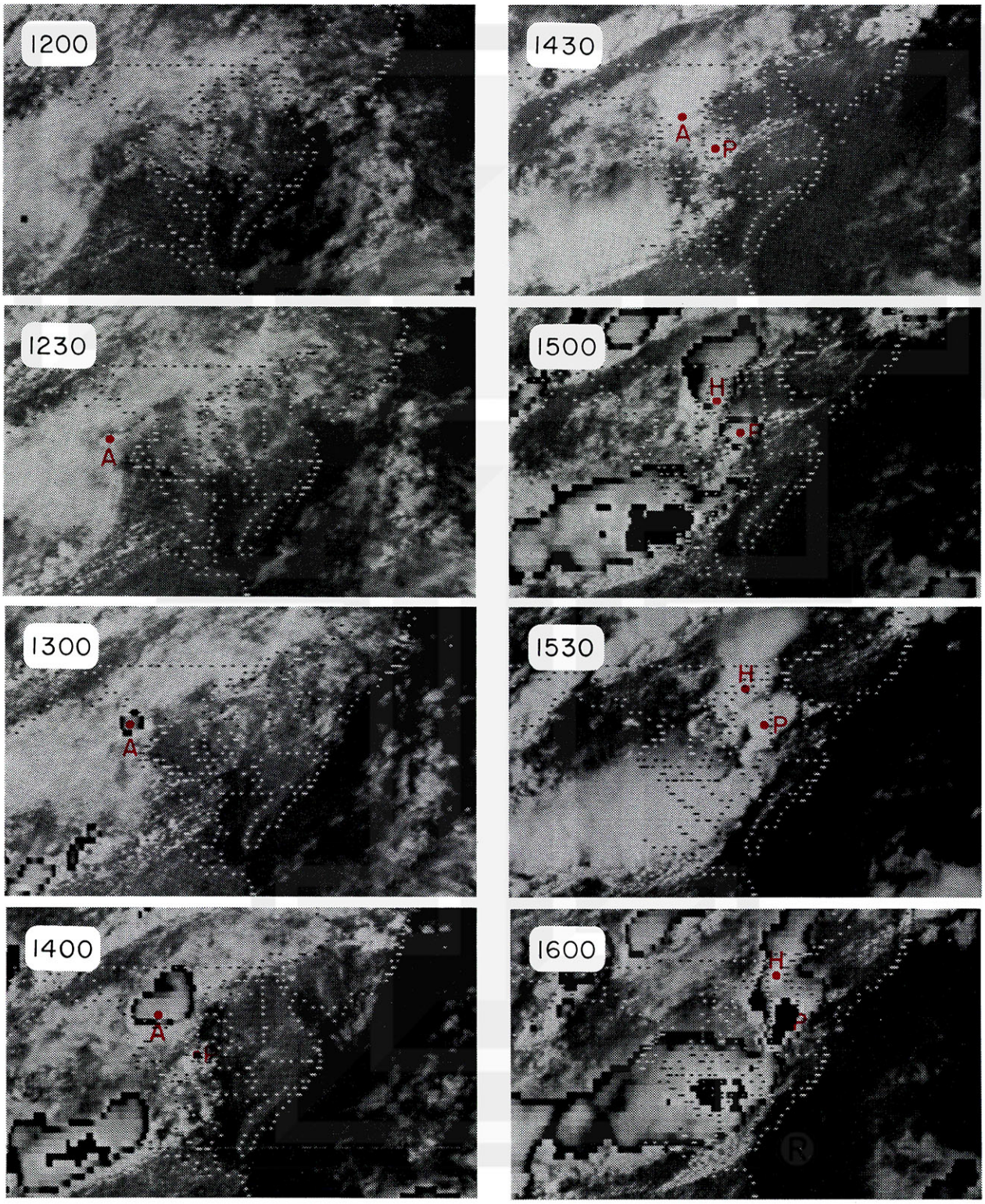

Fig. 9. Andrews(A), Patuxent River(P), and Hillsmere(H) clouds (red).

In an attempt to map the fields of cloud-top temperatures with the highest possible resolution, the IR temperatures of all pixels were printed out on scan line vs. pixel coordinates. IR isotherms were then contoured manually at 2°C intervals.

Cloud-top temperature at 1230 EDT in Fig. 10 is shown with 2°C isotherms. No isotherms above 0°C are included in the map. The Andrews cloud, identified as a towering cloud in Fig. 9, is characterized by -20°C temperature. Due to the existence of extensive middle and high clouds, detailed isotherms failed to close up the relatively warm towering cumulus.

At 1300 EDT, the Andrews cloud grew vertically and the temperature dropped to -53°C (see Fig. 11). For obtaining IR maps, all pixels were plotted at sea-level locations by projecting the satellite-cloud vector all the way to sea level. Such a projection moves the subpixel point away from the true geographic position. The apparent top in the figure denotes the sea-level location while the true top denotes the location directly beneath the cloud top.

1400 EDT map in Fig. 12 shows -57°C temperature of the Andrews cloud with its true top located to the north of the AFB. The Patuxent River cloud with -39°C temperature has appeared at this time.

30 minutes later, at 1430 EDT, the top of the Andrews cloud flattened, showing signs of weakening. This is the time when Patuxent River radar pictures began showing the drift-away anvil cloud.

At 1500 EDT, a significant cold cloud top crossed Chesapeake Bay. It is very likely that the Hillsmere damage by a microburst occurred when this cloud moved over the area. The Patuxent River cloud kept growing, reaching -59°C at this time.

The Patuxent River cloud (-62°C) at 1530 EDT became colder than the weakening Hillsmere cloud (-57°C). So far, no report of high wind was received from beneath the Patuxent River cloud in spite of the fact that this cloud appears to be the more promising.

A line-by-line printout of pixel temperatures at 1400 EDT is shown in Fig. 16. The superimposed blue area is the 1404 EDT echo, scanned with 10° elevation. The coldest cloud tops (-57°C) are seen far to the north of the high-altitude echo, because isotherms were projected to sea level.

Isotherms in Fig. 17 were drawn by adjusting the isotherm positions based on the height-temperature relationship. Such an adjustment shifts isotherms from their apparent positions to the true positions. It should be noted that the echo position and the cold cloud positions are rather close to each other. For detailed analysis of local storms such as these, we have to shift isotherms from apparent to true positions. Otherwise, a tall cloud near Andrews could fictitiously be located over Washington, D.C.

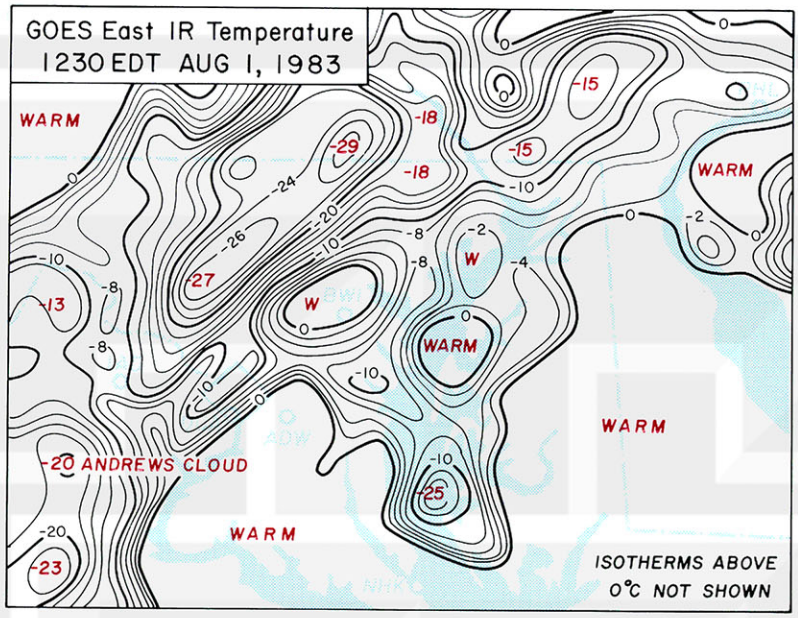

Fig. 10. Distribution of infrared (IR) temperature over the Washington D.C. area depicted by GOES East radiometers. Isotherms were contoured at 2° intervals. The first indication of the Andrews cloud in towering cumulus stage, is characterized by -20°C cloud-top temperature.

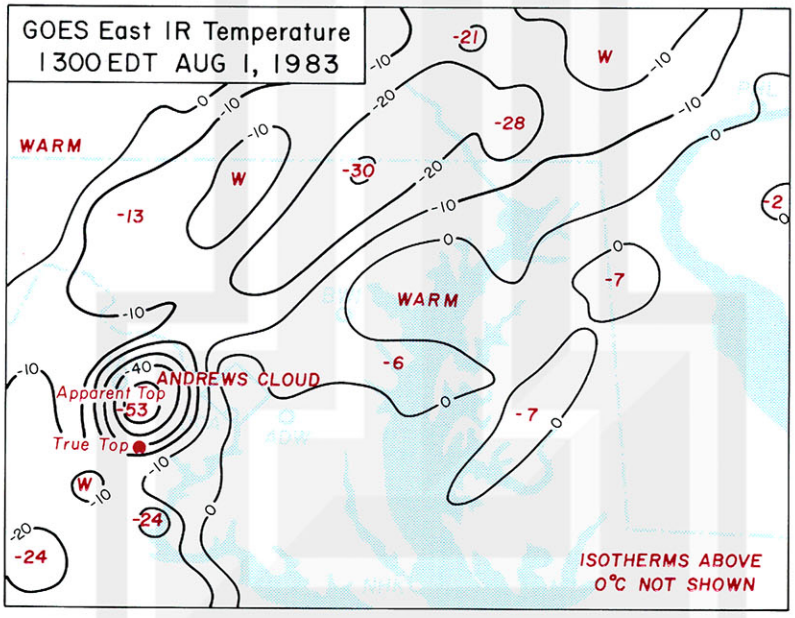

Fig. 11. Andrews cloud with its -53°C temperature projected to sea level. Because of approximately 45° viewing angle of the satellite, the true location of the coldest cloud top is closer to the satellite subpoint. This map includes both apparent and true locations. Isotherms are contoured at 10°C intervals instead of 2°C because of the tight temperature gradient.

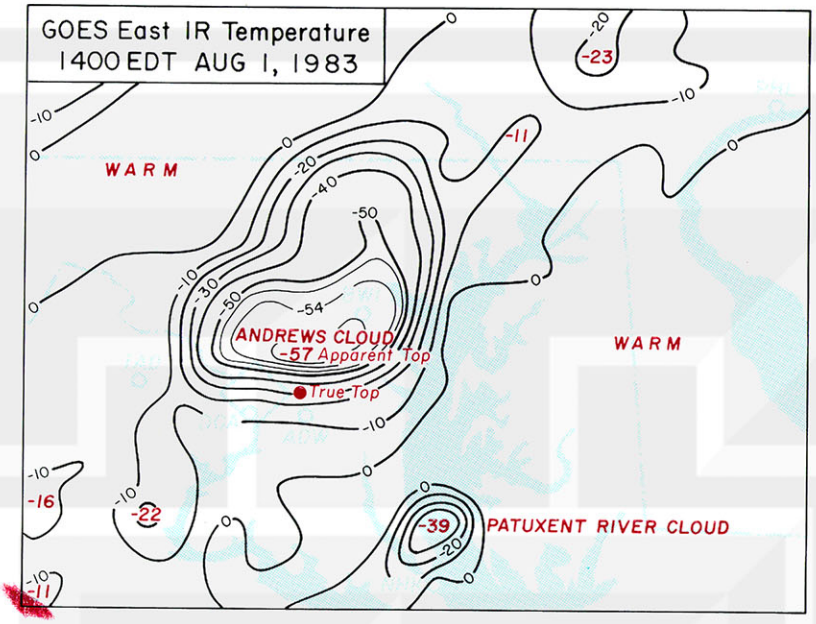

Fig. 12. Isotherms of Andrews cloud at the microburst time. The true top of the -57°C cloud is located to the north of Andrews AFB.

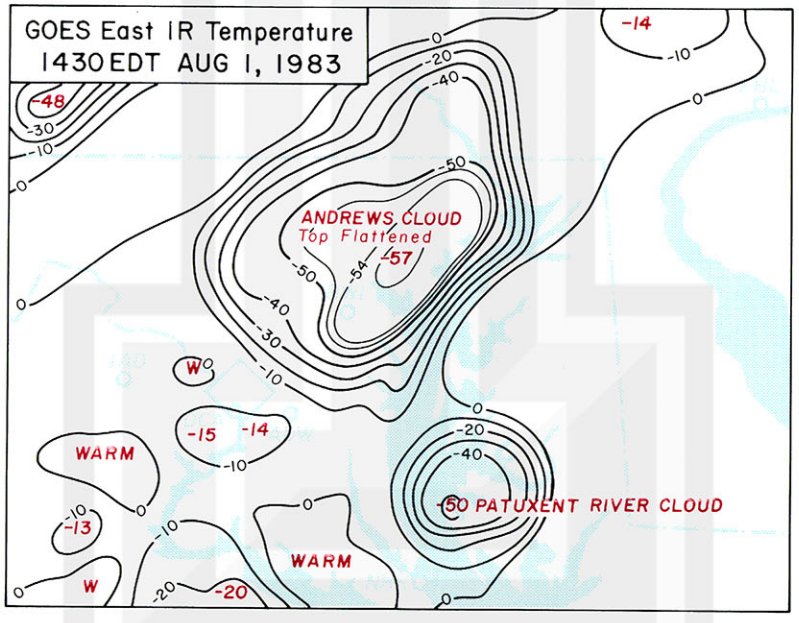

Fig. 13. Cloud-top temperature approximately 20 minutes after the peak microburst wind. Temperature became rather uniform, suggesting that the top of the parent cloud was flattening.

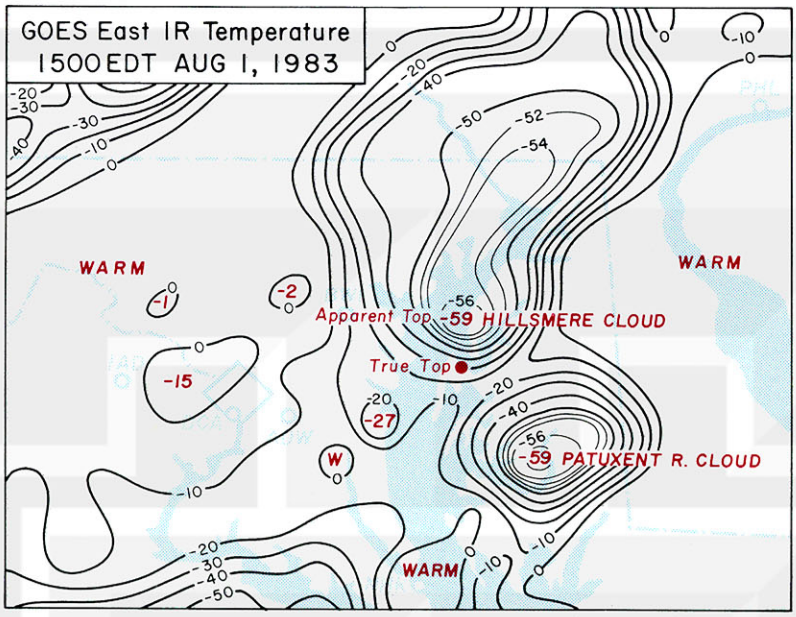

Fig. 14. IR temperature field of the Hillsmere cloud as it was moving away from the damage area just to the south of Annapolis, Md. The coldest cloud top is seen on the east bank of Chesapeake Bay.

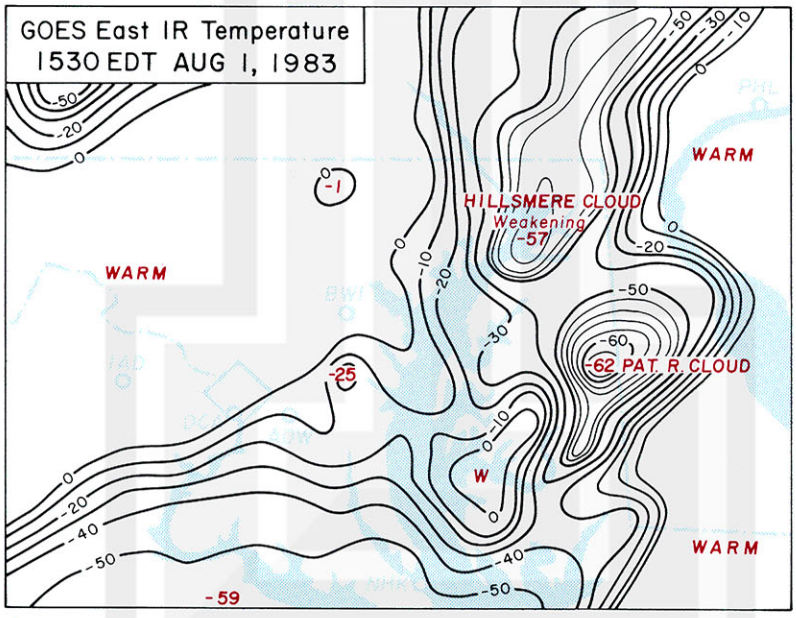

Fig. 15. Hillsmere cloud in its weakening stage and Patuxent River cloud at the mature stage with -62°C cloud-top temperature. So far no report of damaging winds was received from beneath the Patuxent River cloud.

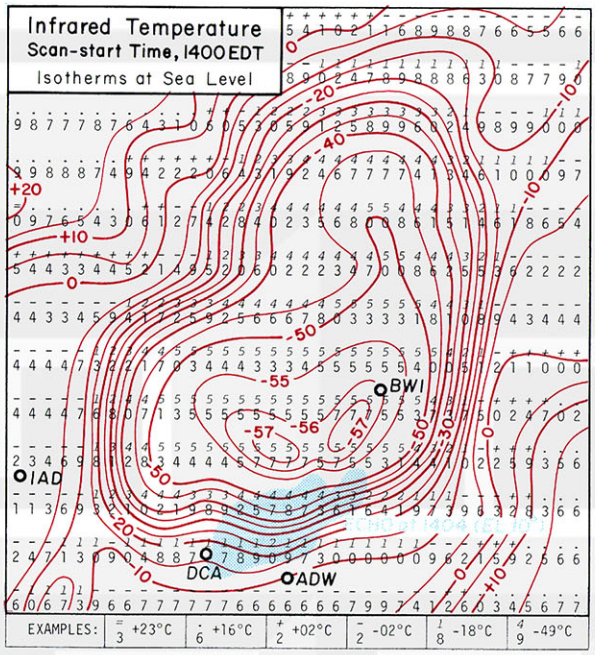

Fig. 16. Pixel by pixel printout of the cloud-top temperature at the time of Andrews AFB microburst. Due to the 45° zenith angle of GOES East, IR pixels projected to sea level shift northward from the true pixel subpoint. This is why cold cloud tops are seen far to the north of the radar echo.

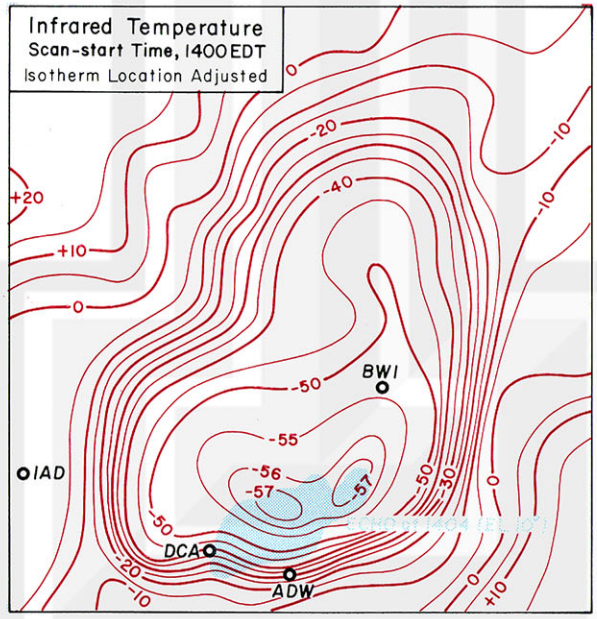

Fig. 17. Field of cloud-top temperature adjusted by shifting each isotherm toward the subsatellite point as much as the height of the isotherm temperature above the surface. Such an adjustment improves the echo-temperature relationship significantly.

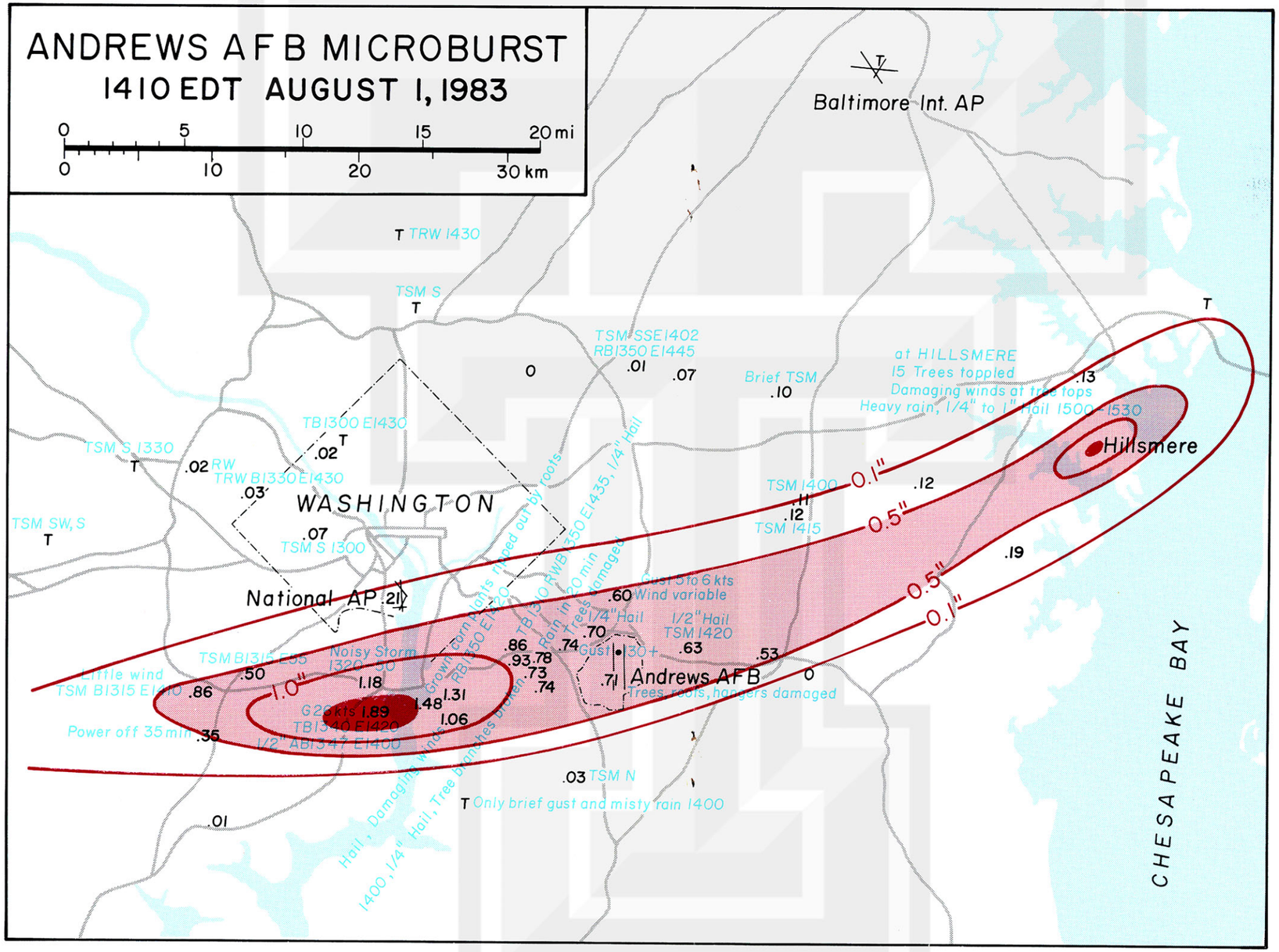

Distribution of wind damage and rainfall beneath the path of the parent cloud of the Andrews Air Force Base microburst on August 1, 1983. Observational data for completing this map were supplied by Stephen D. Ambrose, Hydrologic Research Laboratory of the National Weather Service, and Linwood F. Whitney, Jr., Meteorological Satellite Laboratory of the National Environmental Satellite, Data, and Information Service.

5. UPPER-AIR SOUNDINGS FROM DULLES AIRPORT

Both morning and afternoon soundings made at Dulles Airport are presented in Fig. 18. These soundings were six hours away from 1410, the time of the Andrews microburst. Nevertheless, their basic characteristics did not change much during the whole day.

Unlike typical soundings during JAWS (dry area) microbursts, Andrews AFB (wet area) on August 1 was characterized by the high humidity environment and insignificant instability. There were two dry layers (5-6 and 8-9 km levels) in the morning and one dry layer (4-5 km level) in the afternoon. These dry layers are rather usual in the Washington, D.C. area, however.

Due to insignificant instability, the top of the spreading anvil was located at the base of a stable layer approximately 2 km below the tropopause. Furthermore, the echo-top height remained at 42,000 ft throughout the activity time. It is still a mystery how such an innocuous thunderstorm induced the violent microburst winds experienced at Andrews Air Force Base.

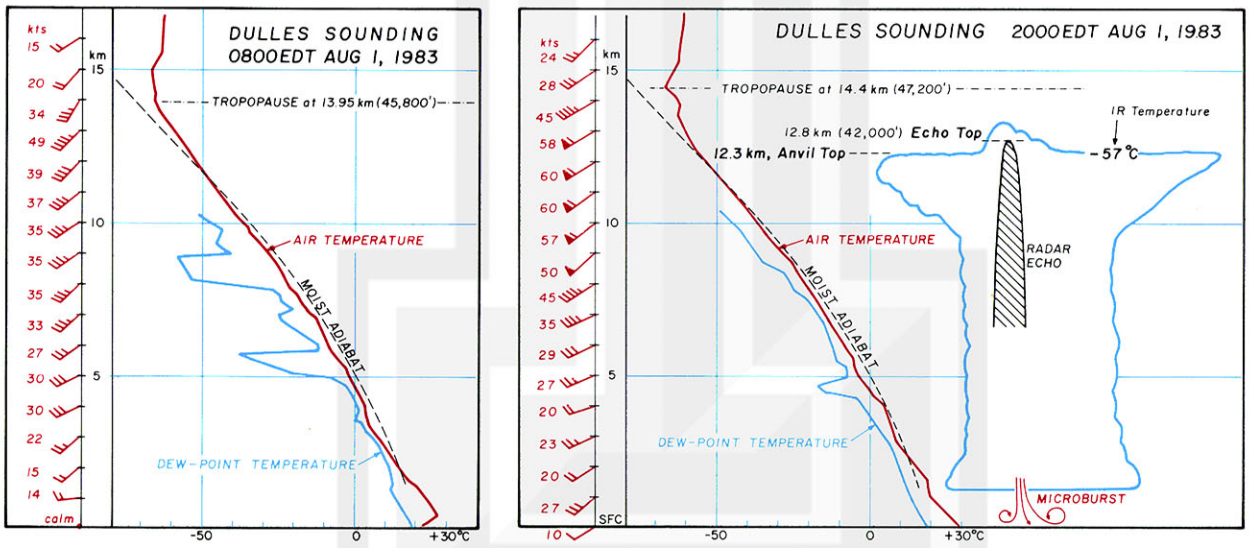

Fig. 18. Dulles sounding at 0800 and 2000 EDT on August 1, 1983. The stratification was relatively stable - nothing like a severe thunderstorm case over the midwest. Lifted indices were only -3 to 4°C. Unlike JAWS microburst environment, layers below 4 km AGL were nearly saturated. Both echo and anvil tops were located below the tropopause. A stable layer, 2 km below the tropopause, apparently prevented the vertical growth of the cloud.

6. LOCAL WEATHER IN WASHINGTON, D.C. AND VICINITY

A small thunderstorm cell at 1233 EDT in Fig. 6 was 64 n.m. away from Andrews AFB (ADW). Although we are not able to confirm the first rain on the ground, the first report of the approaching storm was made at 1315 EDT just to the south of Capital Beltway in Virginia where 0.86" of rainfall was measured.

While approaching the Potomac River the thunderstorm unloaded 1.89" of rain in 40 minutes between 1340 and 1420. 1/2" hail was observed for 13 minutes between 1347 and 1400. However, winds were not strong during the storm; only up to 26 kts gusts were observed.

The fury of the storm was experienced just to the east of the Potomac where 1.48" rainfall was measured by Bonnette. It was a violent thunderstorm and his yard was covered with leaves and twigs. Some nearly matured corn plants were ripped out by the roots. It is very likely that the first microburst from the parent cloud descended near his site. The Alexander site (1.06" rainfall) also reported damaging winds, hail, and thunder. The Frederick site (1.31" rainfall) recorded 30 minutes of rain between 1350 and 1420.

Due to the lack of reporting sites to the east of these three sites, we are not able to assess whether there had been a separate microburst between the Potomac and Andrews AFB. The Filippelli site (0.73" rainfall) reported a heavy thunderstorm at 1400 with strong winds, rain, and 1.4" hail. Some tree branches were broken.

The Oprendek site, 2 miles east of the Base, recorded 0.63" rainfall with 1/2" hail during the thunderstorm at 1420. In general, rainfall amount decreased from the Potomac River eastward.

The width of the 0.5" rainfall was 5 miles on the Potomac. Its width was maintained until passing over Andrews AFB. Thereafter, the width gradually narrowed to about 3 miles before reaching Hillsmere, a community just to the south of Annapolis. To the south of the 0.5" isohyet, rainfall decreased rapidly to near zero. To the north, however, rainfall decreased gradually because of the anvil blowoff which extended northward from the storm's core region.

As shown in the centerfold map, Hillsmere was hit by a localized wind, probably a small microburst. 15 trees were uprooted; twigs and branches were ripped off trees. Nonetheless, the damaging winds stayed a certain height above the ground; the cornfields near the toppled trees were not affected by the wind. The Hillsmere storm was accompanied by 1/4" to 1" hail. Rain was so heavy that local residents estimated the rainfall in excess of one inch during this brief windstorm.

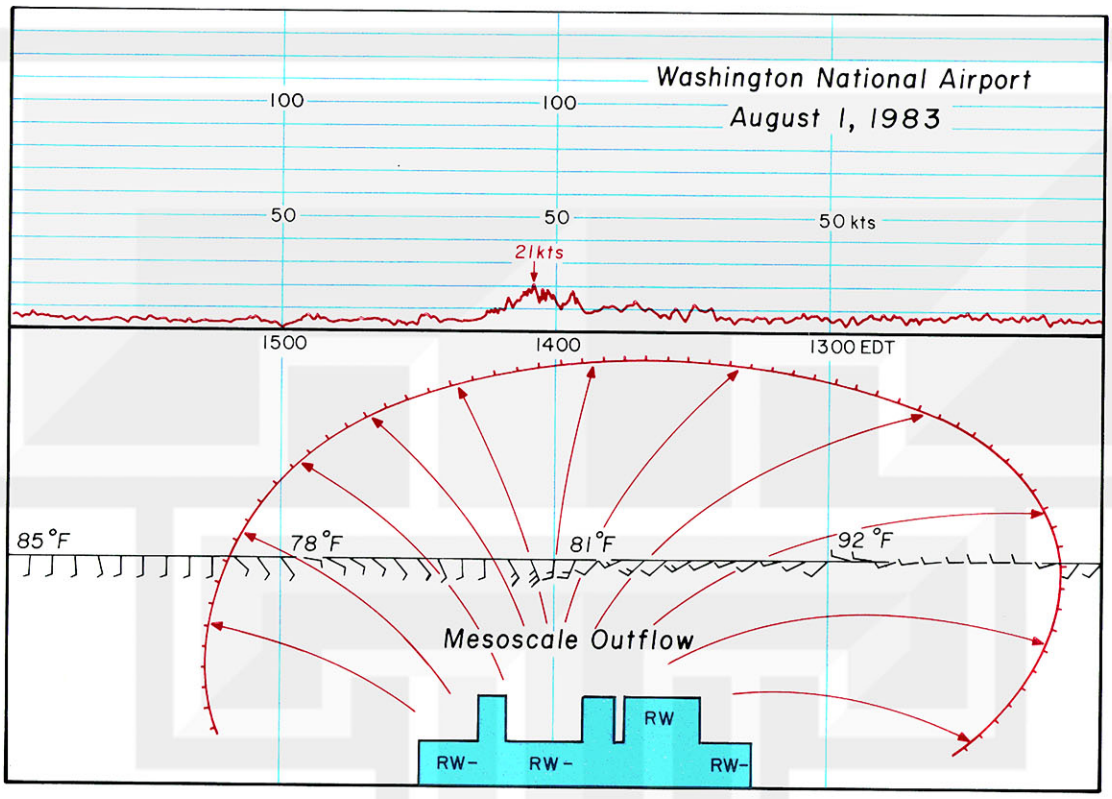

Fig. 19. Time cross section of meteorological parameters observed at Washington National Airport (DCA) located 4.5 miles to the north of the rainfall center line extending from the south of Capital Beltway to near Annapolis, Md. (see centerfold map).

Surface Weather Observations at Washington National Airport

Time EDT	Sky and Ceiling in 100 ft	P mb	T °F	Td °F	Dr deg	Sp kts		Remarks
1326	E50BKN 110OVC				27	11	TRW-	TB25 W MOVG SE OCNL LTGCG
1351	E50BKN 100OVC	190	81	70	24	11	TRW+	TB25 SE-W MOVG E OCNLLTGCG RB16
1402	35SCT E55BKN 100OVC				18	17	TRW-	T NE-SW MOVG E OCNL LTGCG
1436	50SCT E100BKN 250BKN				14	05		TE33 MOVD E CB NE-SE MOVG E

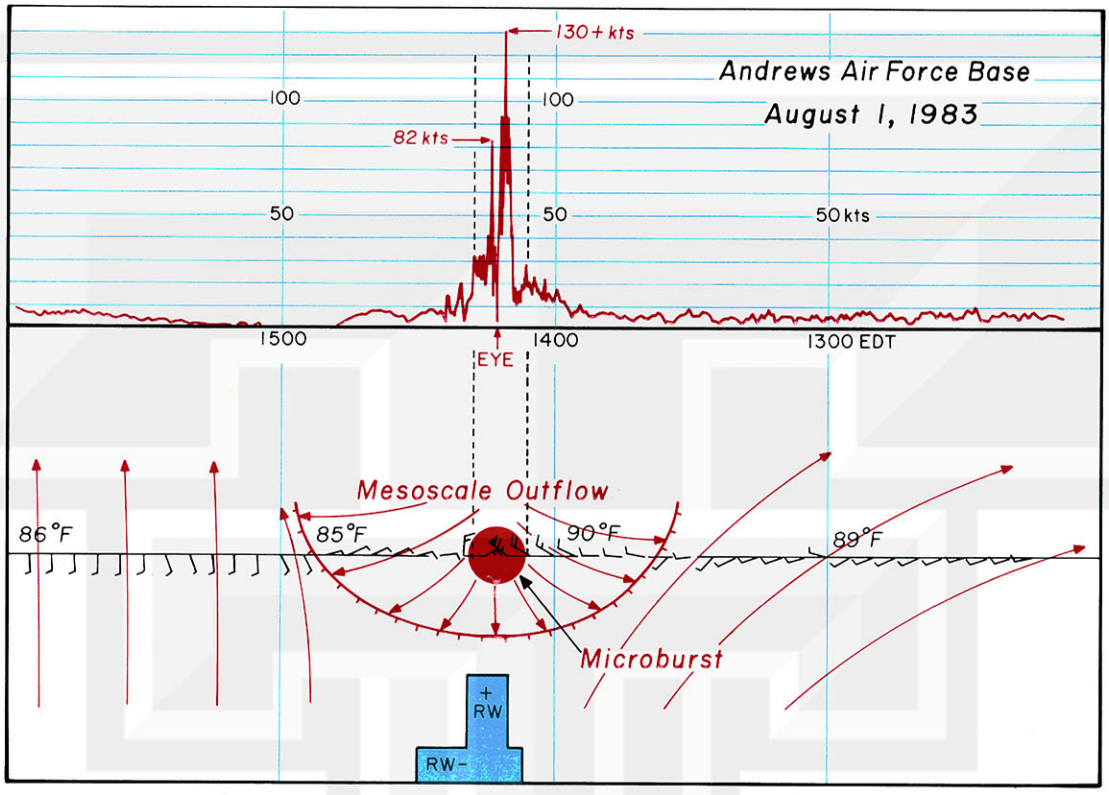

Fig. 20. Time cross section of meteorological parameters observed at Andrews AFB located just to the south of the rainfall center line (see center-fold map). Note that the area of the microburst (red circle) is significantly smaller than the overall area of the mesoscale outflow which affected the Air Force Base.

Surface Weather Observations at Andrews Air Force Base

Time EDT	Sky and Ceiling in 100 ft	P mb	T °F	Td °F	Dr deg	Sp kts		Remarks
1355	20SCT E30BKN 220OVC	181	90	69	26	08	T	T SW-NW MOVG ENE OCNL LTGICCCCG
1405	7SCT E25BKN 220OVC				30	14	T	T OVHD MOVG ENE OCNL LTGICCCCG Gust23
1407	7SCT E20BKN 220OVC				28	18	TRW-	T OVHD MOVG ENE FQT LTG ICCCCG Gust 27
1410	W1X				E30	10	TRW+	T OVHD MOVG ENE OCNL LTGCCCG A 1/4 Gust50
1419	W5X				34	07	TRW-	T OVHD MOVG ENE OCNL LTGICCCCG A1/4" G14

Fig. 21. One of the Hillsmere streets blocked by tree branches in the wake of a micorburst. (Photo by Jim Burke, Capital-Gazette, Annapolis, Md)

Fig. 22. Snapped and uprooted trees at Hillsmere. (Photo by Jim Burke) The microburst was accompanied by 1/4" to 1" hail. Power lines downed and 15 trees toppled.

7. MODEL OF MICROBURSTS

A microburst consists of a downflow and an outflow which are smoothly joined into a system of three dimensional airflow. Similar to the Bernoulli's flow, the downflow provides the outflow with the energy required for it to spread out violently.

Air should be calm at the stagnation point beneath the downflow where the total pressure provided by the downflow can be measured as the stagnation pressure. Pitot tubes with their openings pointing toward the impinging flow will also measure the total pressure.

When the outflow air gains speed as it flows out of the stagnation area, the static pressure decreases in such a way that the total pressure is conserved. Thus we write

$$P_T = P_s + \frac{1}{2}\rho V^2$$

where P_T denotes the total pressure, P_s the static pressure, V the speed of the outflow air. Since microbursts are low-altitude phenomena, we may assume that ρ is constant. Using 1.18 kg/m^3, the density of air at Andrews AFB during the microburst, the difference between the total and the static pressure is computed from

$$\Delta P = P_T - P_s = \frac{1}{2}\rho V^2 = 0.00156\ V^2 \text{ mb}$$

where V is in kts and P in mb.

Table 3. $\Delta P = P_T - P_s$ computed as a function of the outflow speed V. (V in kts and P in mb)

Outflow speed	0	2	4	6	8 kts
10s kts	0.2	0.2	0.3	0.4	0.5
20s	0.6	0.8	0.9	1.1	1.2
30s	1.4	1.6	1.8	2.0	2.2
40s	2.5	2.8	3.0	3.3	3.6
50s	3.9	4.2	4.5	4.9	5.2
60s	5.6	6.0	6.4	6.8	7.2
70s	7.6	8.0	8.5	9.0	9.5
80s	10.0	10.5	11.0	11.5	12.1
90s	12.6	13.2	13.8	14.4	15.0
100s	15.6	16.2	16.9	17.5	18.2
110s	18.8	19.6	20.2	21.0	21.7
120s	22.4	23.2	24.0	24.7	25.6
130s	26.3	27.2	28.0	28.8	29.7
140s	30.5	31.5	32.3	33.3	34.2

Outflow speeds of weak microbursts can be induced by a relatively small total pressure. As the outflow speed increases, however, the total pressure required to accelerate the outflow winds becomes so large that the total pressure provided by an ordinary downflow becomes insufficient, provided that a downflow speed in excess of 100 kts can be justified.

On the other hand, the Dulles soundings on the day of the Andrews AFB microburst appear to be too small to generate an unusually large downflow speed which could generate the total pressure required to induce outflow winds over 100 kts.

To overcome this difficulty, we have to look for a special mechanism by which the outflow air can achieve its ultimate wind speed without relying solely on the total pressure provided by the downflow. In other words, an ordinary downflow, by itself, cannot generate the Andrews AFB type of intense outflow.

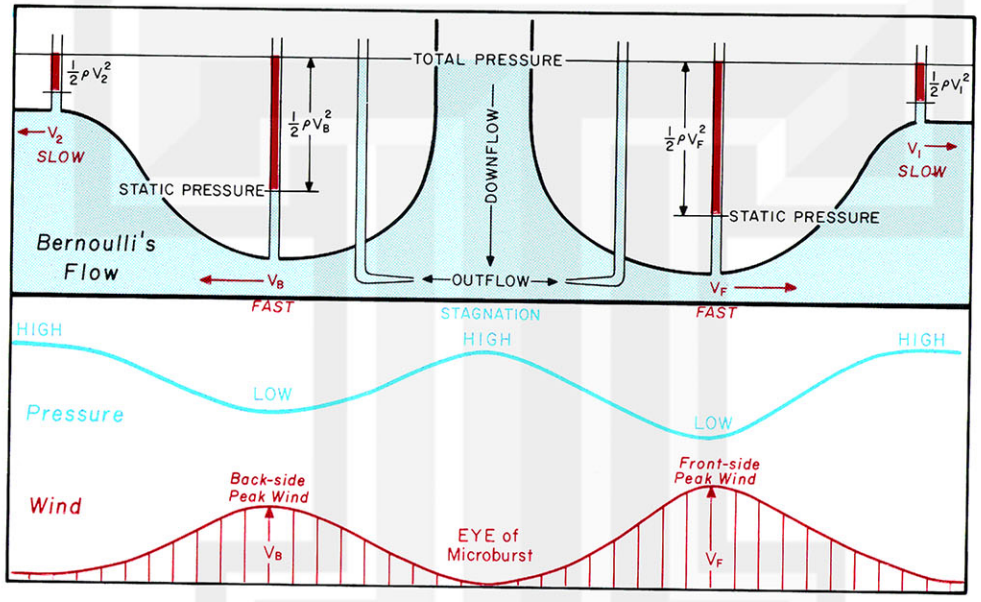

Fig. 23. Schematic diagram showing the conservation of total pressure. The static pressure of the outburst air decreases as wind speeds increase.

A sequence of pictures (see Fig. 24) taken during the JAWS Project reveals the existence of a tight-core vortex with its horizontal axis. The red vectors superimposed upon the last picture in the sequence show that the downflow air was swirling into the vortex while probably conserving its angular momentum. A spin-up circulation can be expected because the horizontal vortex ring around the microburst should stretch gradually. An intense circulation generated a counter circulation at the top of the horizontal vortex.

Fig. 24. A sequence of pictures showing the curling motion of the dust cloud behind the leading edge of a microburst outflow. Looking southeast from JAWS CP-3 site on July 15, 1982. (Photo by Brian Waranauskas)

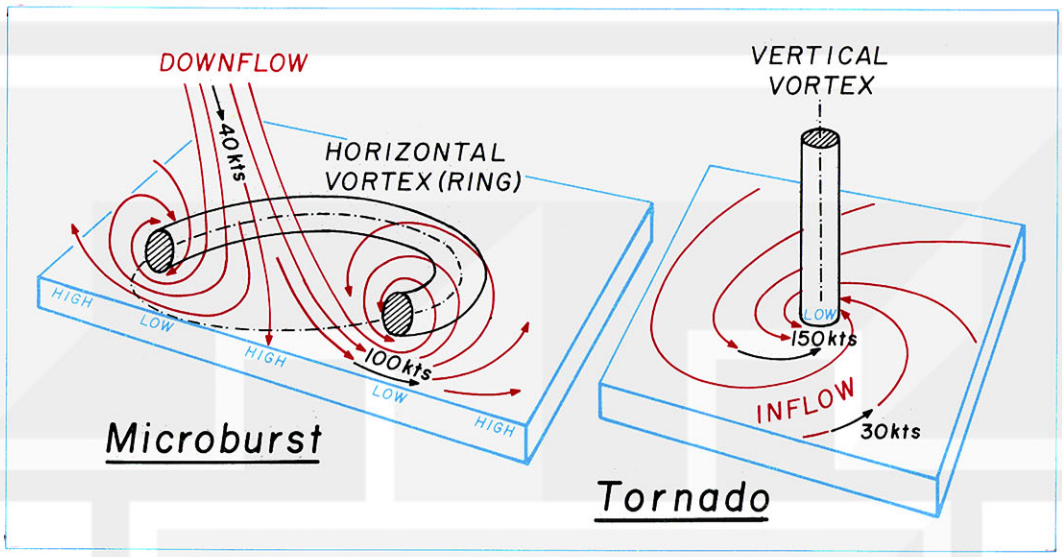

Fig. 25. Similarity between "Tornado" and "Microburst". The inflow wind in a tornado increases the wind speed during its approach toward the vortex core with the vertical vortex axis. The downflow in a microburst increases the wind speed during its approach toward the vortex core with horizontal vortex axis. In both storms, the stretching action of the vortices provides the mechanism for the spin-up rotation.

A model of a microburst presented in Fig. 25 consists of a downflow surrounded by a ring of horizontal vortex. For explaining the mechanism of accelerating the outflow air, a tornado model on the right side will be explained first.

An extremely fast tornado wind speed is located around the core. It could be 150 kts or even higher. However, we do not find such a high speed anywhere within the inflow region. The tornado wind speed simply increases as the inflow air spirals into the low pressure area while maintaining the angular momentum. The low pressure core is maintained by the stretching of the swirling winds.

Likewise, the 100 kts outflow beneath the horizontal vortex can be achieved by the spin-up motion made possible by the stretching deformation of the ring vortex. Thus the downflow speed can be significantly less than the speed of the outflow wind. In other words, the downflow can generate much faster outflow winds with the help of the stretching ring vortex.

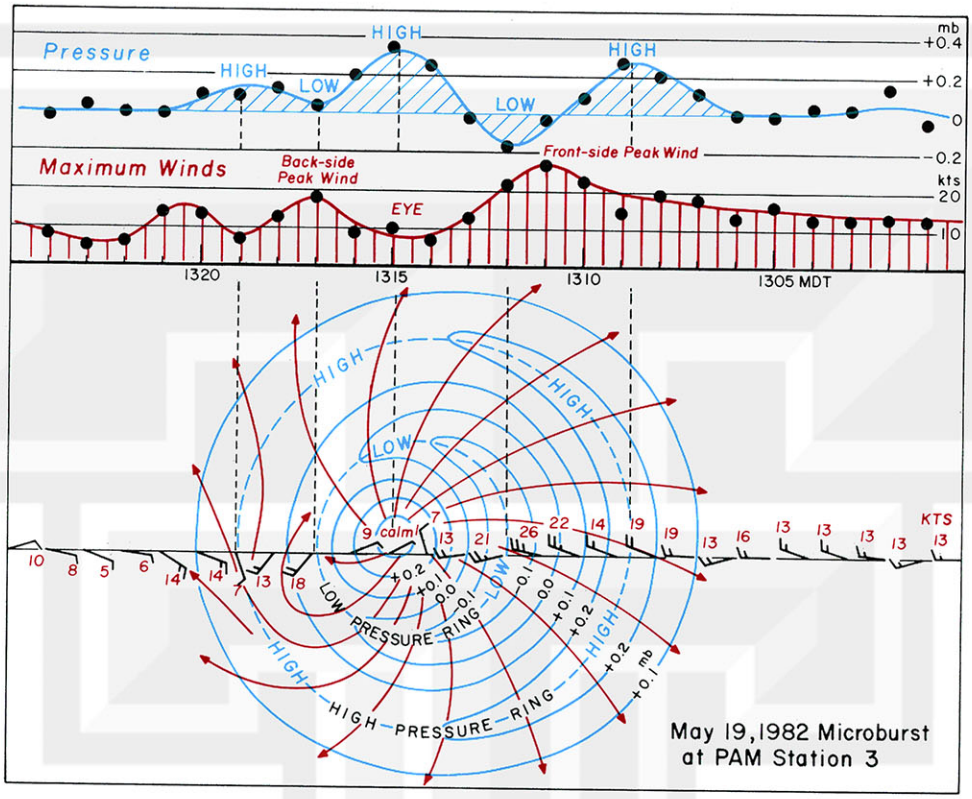

Fig. 26. JAWS microburst on May 19, 1982 which passed almost directly over PAM Station No.3. Three maxima and two minima in the pressure profile were recorded during the passage.

Fig. 26 shows wind and pressure distributions of the May 19, 1982 microburst which passed almost directly over PAM Station No. 3. While fixing a flat tire on the way to JAWS CP-3 Doppler radar east of the PAM station, the author saw a microburst over this station. Upon arrival at the radar, it was learned that the radar was not scanning the microburst, because nobody at the radar was aware of this microburst which moved over the radar.

Examination of PAM data at a later time revealed that Station No. 3 was almost directly beneath the microburst. There was a dome of high pressure at the microburst center. The central high pressure was surrounded by a ring of low pressure where the wind speed reached a peak. The low pressure ring was encircled by a high pressure ring and a significant deceleration of the outflow winds took place between low and high pressure rings.

Unlike the simple pressure field of a tornado, which is characterized by low pressure around its axis of rotation, pressure distribution in a microburst is rather complicated.

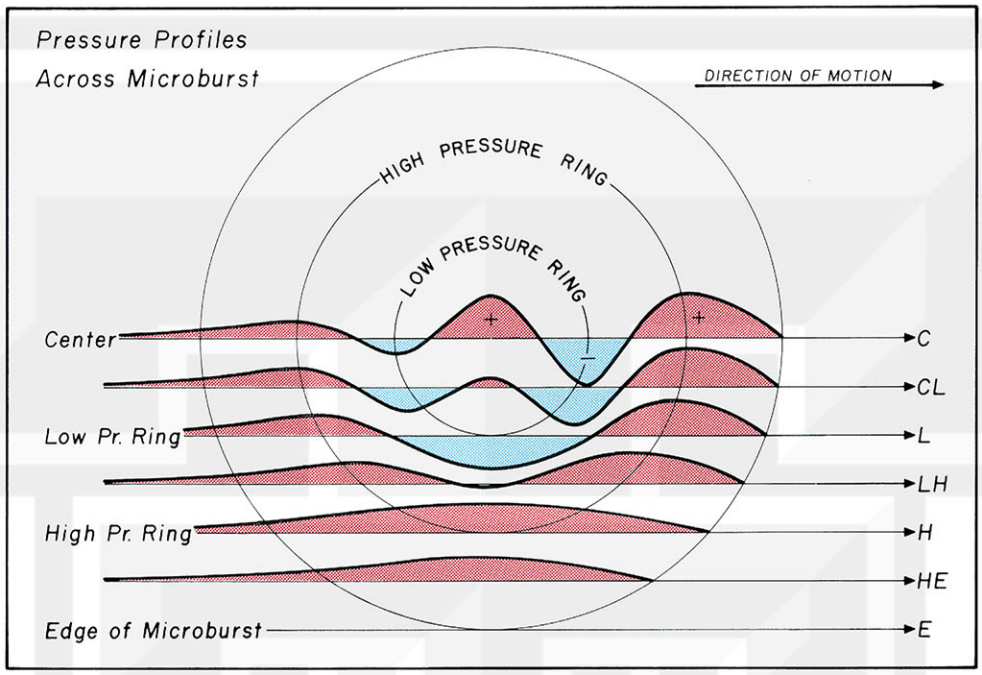

Fig. 27. Pressure profile through a microburst which is traveling from left to right. Profiles vary significantly with the location of barograph relative to the path of the microburst center.

The high pressure dome at the center of a microburst is induced by the stagnation pressure. The central high pressure dome is encircled by a low pressure ring toward which outflow winds are accelerated. Upon reaching the highest wind speed at the low pressure ring, outflow winds decelerate toward the high pressure ring which encircles the low pressure ring. Outside the high pressure ring, pressure drops to the environmental level, often forming a small arc of pressure-jump line on its advancing side.

Fig. 27 shows schematic pressure profiles across a microburst. In relation to the microburst center line C goes through the microburst center. Line L touches the edge of the low pressure ring and line H, the edge of the high pressure ring. Line E touches the edge of the microburst, and little or no pressure change occurs along the line.

There is always the chance that a profile line will go through between lines C, L, H, and E. These in-between lines are identified by combined letters, CL, LH, and HE. Pressure profiles in Fig. 27 were drawn along these seven lines.

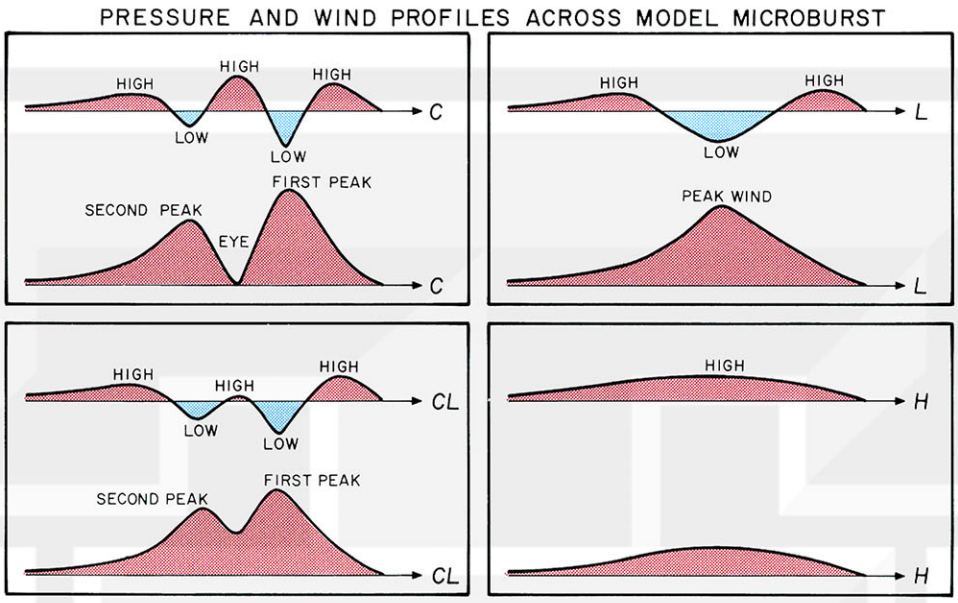

Fig. 28. Pressure and wind profiles at four different locations. C -- Center passes directly over the station. L -- Edge of the low-pressure ring passes over the station. LC -- Somewhere between L and C. H -- Edge of the high pressure ring passes over the station.

Based on the PAM data, NIMROD (1978) and JAWS (1982) projects identified 50 and 186 microbursts respectively. Variations of both pressure and wind during these microbursts were examined in an attempt to determine the location of the PAM station relative to the microburst center.

Table 3. Location of PAM stations relative to the center of microbursts. None of the NIMROD stations was at the microburst center.

NIMROD Project								
Lines	C	CL	L	LH	H	HE	?	Total
No of microbursts	0	1	13	13	9	4	10	50
(in %)	(0)	(2)	(26)	(26)	(18)	(8)	(20)	(100)

JAWS Project								
Lines	C	CL	L	LH	H	HE	?	Total
No of microbursts	2	8	89	23	20	5	39	186
(in %)	(1)	(4)	(48)	(12)	(11)	(3)	(21)	(100)

In general, wind speed and surface pressure in microbursts are negatively correlated, because winds accelerate from the central high pressure dome toward the low pressure ring. As pressure increases toward the high pressure ring, wind speeds decrease. Fig. 28 presents four cases of wind-pressure relationship expected to occur along lines C, CL, L, H. Existence of these cases has been confirmed in NIMROD and JAWS microbursts.

8. ANDREWS AIR FORCE BASE MICROBURST

It is very difficult to determine the two-dimensional distribution of wind and pressure on the basis of one anemometer trace and a barogram recorded at two sites separated by approximately one mile. The so-called time-space conversion method appears to be the only means of constructing a two-dimensional map.

Under the assumption that the front-side and the back-side maximum winds would be equal in strength and opposite in direction if the microburst were not traveling, the difference in the maximum winds was used in determining the traveling velocity of the microburst. The speed was obtained from

$$\text{Traveling speed} = \frac{1}{2}\,(\text{front-side max. wind} - \text{back-side max. wind})$$

$$= \frac{1}{2}\,(112 \text{ kts} - 62 \text{ kts}) = 25 \text{ kts}$$

Making use of this traveling speed, the time-domain variations of both wind and pressure were converted into the space-domain distribution in Fig. 29. The microburst map, thus analysed, includes both wind field (in red) and pressure field (in blue).

It is seen that the outflow winds from the calm region (eye) of the microburst intensify toward the low pressure ring which is one mile in diameter. Their peak wind speeds are reached at the low pressure ring. Thereafter, the outflow speeds decrease toward the high pressure ring approximately two miles in diameter.

Apparently, the barograph at the Base Weather Station remained outside the high pressure ring. It recorded a rapid rise followed by a general decrease (see Fig. 1).

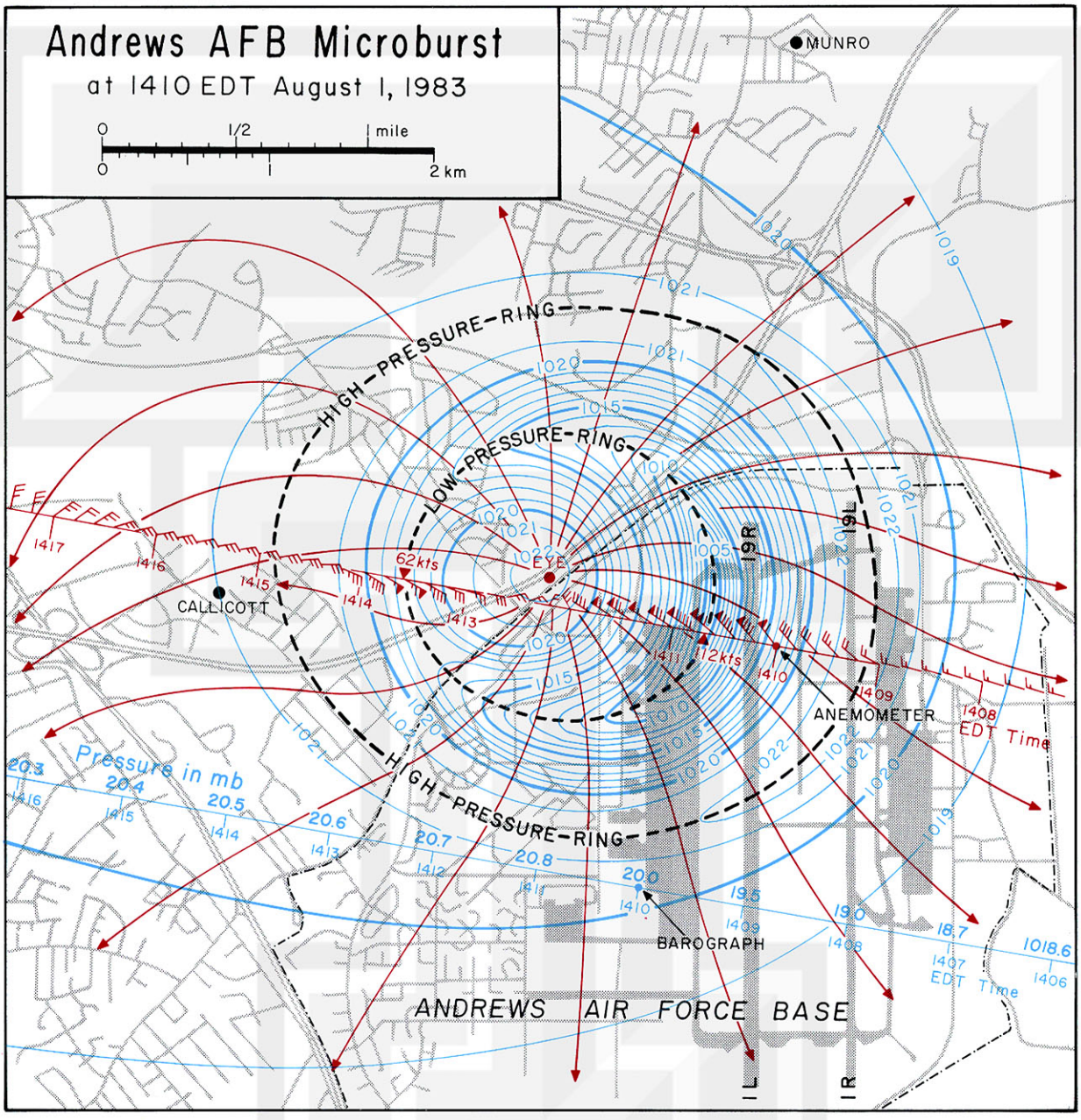

Fig. 29. Wind and pressure fields of Andrews AFB microburst at 1410 EDT on August 1, 1983. Pressure field was estimated through time-space conversions of the wind data along with the model of the pressure field in Fig. 26. Pressure measured at the Base Weather Station, approximately 1 mile south of the microburst center, showed only one peak (see Fig. 1).

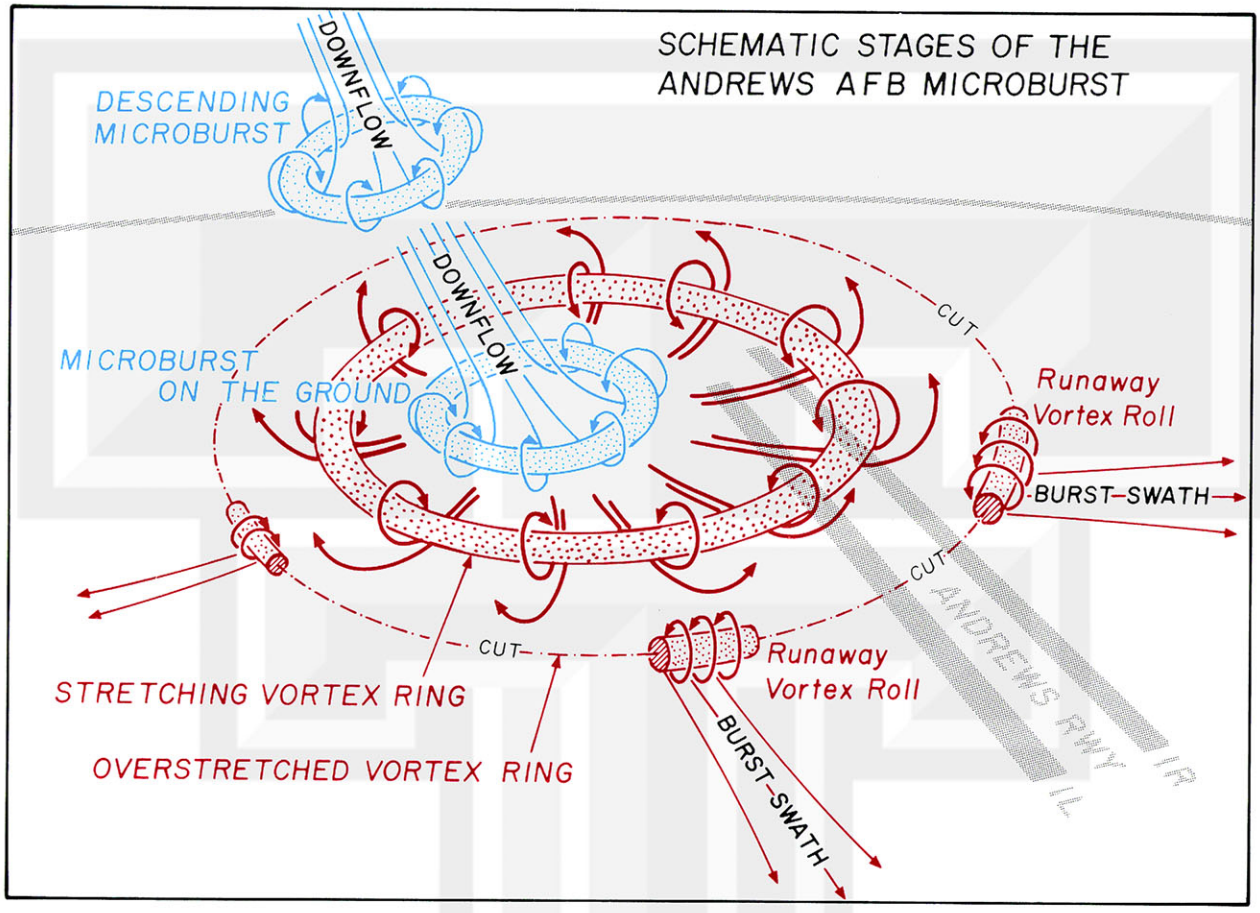

Fig. 30. Four stages of Andrews AFB microburst. They are:

1st Stage (DESCENDING STAGE) Midair microburst descends.

2nd Stage (CONTACT STAGE) Microburst hits the ground.

3rd Stage (MATURE STAGE) Stretching of the ring vortex intensifies storm.

4th Stage (BREAKUP STAGE) Runaway vortex rolls induce burst swaths.

An attempt was made to describe the Andrews AFB microburst in three-dimensional space (see Fig. 30). During the 1st stage, the microburst was descending toward the Base. The 2nd stage was the contact stage in which the microburst hit the ground near Capital Beltway. During the 3rd stage, the vortex ring was stretching rapidly, while advancing toward the east-southeast. The wind speeds reached their peak values during this stage.

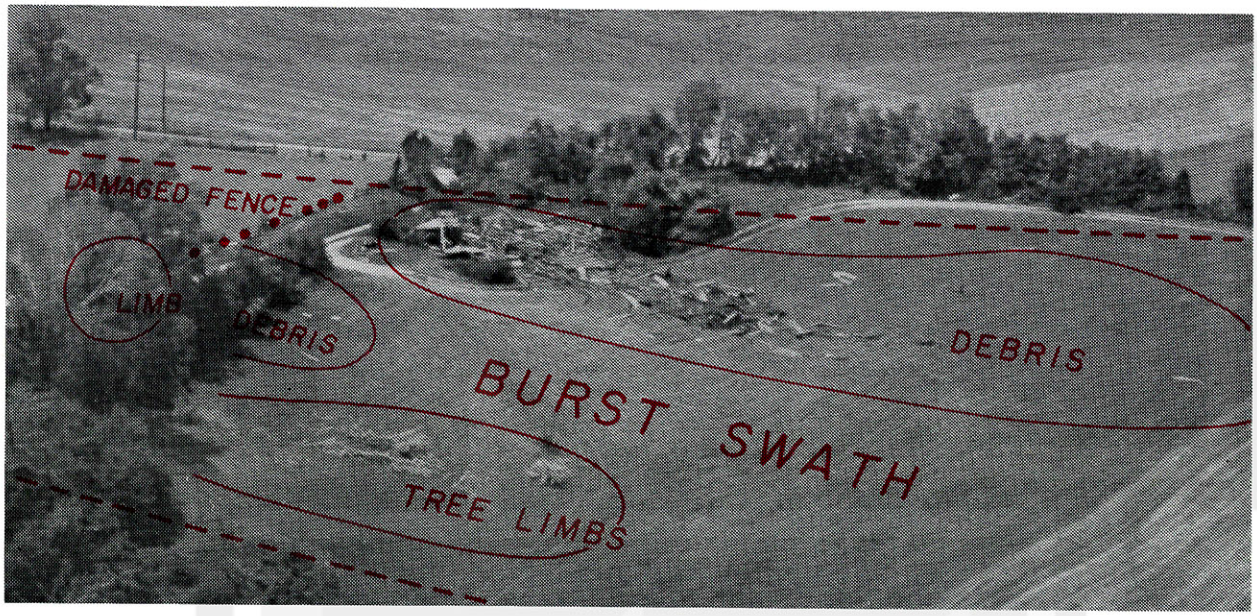

Fig. 31. A band of damage inside the "Burst Swath" located to the east-northeast of Andrews Air Force Base. This picture was taken east of the 3900 block of Mellwood Road off the north branch of Cabin Branch. The exact orientation of the debris is not certain; however, the photographer believes that it is oriented from the west-southwest. (USAF Photo)

When the vortex ring overstretched, the ring was cut into small vortex rolls called in this paper "runaway vortex roll". It is speculated that such a fast-moving vortex with horizontal axis could induce damaging winds beneath its path.

Numerous cases of burst-swath damage have been documented elsewhere. A burst-swath like damage was photographed by USAF in the wake of the Andrews AFB microburst (see Fig. 31).

CONCLUSIONS AND RECOMMENDATIONS

On the basis of his analysis of NIMROD and JAWS data, the author concludes that Andrews AFB microburst did induce the fastest wind ever recorded. Of 236 microbursts which had been studied, only two were documented by PAM stations located within 0.3 mile of the microburst center. The Andrews anemometer was located within 0.1 mile of the center, recording the 2 kts wind inside the eye of the microburst.

Andrews AFB microburst was spawned by a small thunderstorm, the top of which was located 3 n.m. northwest of the Base when the microburst hit the runway area. The thunderstorm moved toward the east-northeast, but the microburst shot out of the cloud toward the east-southeast, 30 to 40° to the right of the thunderstorm motion.

At the present time, there is no means of detecting the Andrews AFB type of microburst in advance of the onset of high winds on the airport ground. Should an aircraft be caught by strong microburst winds, tailwind, crosswind, downflow, singly or in combination, could result in serious,irreversible consequences.

In order to issue timely warnings of microburst winds, it is necesssry to detect microbursts during their descending stage, not after the contact stage. Since a microburst can descend directly to the runway area, it must be monitored by a Doppler radar located 5 to 20 miles outside the airport. The author urgently recommends that a Doppler radar be placed at a strategic location in the Washington D.C. area, capable of scanning Andrews AFB, Washington National, Baltimore, and Dulles Airports. Meanwhile, the helicopter route between the White House and Andrews AFB should be monitored by such a Doppler radar.

Questions & Answers

Numerous questions have been asked since the author introduced the term "DOWNBURST" and "MICROBURST" in March 1976. Questions presented in this section were selected from those asked by pilots, meteorologists, and my students.

Q: How do you rank the Andrews AFB microburst in terms of storm intensity?

A: As far as I know, the Andrews storm induced the strongest peak wind ever recorded by anemometer. Numerous wind damages in the Base also confirms the intensity of the unusual (top one percent) intensity of this microburst.

Q: Why is the microburst important for aviation?

A: A microburst induces dangerous tailwind, crosswind, and downflow just above the runway height. The storm is very small and short-lived, lasting no more than 5 minutes. It cannot be predicted and it is hard to detect until it becomes too late to fly out. For timely warning, we have to detect microbursts before we descend to the runway area. A midair detection of a microburst is required.

Q: What does a microburst look like from the cockpit?

A: It looks like a localized shower, either heavy or very light. There is no way of judging from the cockpit if the root of the shower is inducing (or will induce) microburst winds.

Q: What is the first indication that I am flying into a microburst?

A: An indication is the unusual increase in the airspeed and aircraft altitude while approaching a shower, which may look either bad or innocuous. Downflow, tailwind, crosswind, and their combinations could be waiting only a few seconds away.

Q: It is best not to fly into a microburst. How early can you detect a microburst which endangers aircraft operations at low altitude?

A: In my view, most of the Denver-type dry microbursts can be detected by a single Doppler radar 2 to 3 minutes before the onset of microburst winds on the ground. The Doppler radar must be located 10 to 30 km away from the runway area in order to detect microbursts in their midair stage. A microburst in a wet area, such as Andrews AFB or New Orleans, is very hard to detect, because no mechanism for microburst formation in wet areas is known.

Q: Do we have reports of microburst-related incidents or accidents since the New Orleans accident in July 1982?

A: Three microbursts (one suspected) occurred inside the airport grounds of Denver's Stapleton, Chicago's O'Hare, and Andrews Air Force Base.

June 1983 at Stapleton *A 727 encountered a strong tailwind shear on runway 35L. Less than a minute earlier, another jet had taken off, reporting nothing unusual. A cumulonimbus overhang extended over the airport with a few raindrops on the windshield. No blowing dust, debris in the air and no LLWSAS warning issued. Lifted off 300 to 500 ft of runway remaining.*

July 1983 at O'Hare *A 727-200 lifted off on runway 32R in very light rain. All of a sudden, aircraft hit a wall of rain and airspeed dropped, accompanied by stick shaker activation. Altitude decreased from between 50 to 100 ft to 15 ft; then it started climbing again. No LLWSAS warning was issued.*

August 1983 at Andrews AFB *Air Force One with the President on board landed at 2:04 p.m. Flight information depicted a thunderstorm west of the airfield moving to the norhteast. An uneventful landing was accomplished on the dry runway. Air Force One was shut down on the ramp when the storm struck at 2:10 p.m. Andrews AFB is not equipped with an LLWSAS system.*

Q: Do microbursts always produce rain on the ground?

A: The answer to this question is no. 85% of the JAWS microbursts produced no rain on the ground (dry microburst) and 48% of the NIMROD microbursts were dry.

Q: How much rain do you expect in a very wet microburst?

A: Andrews AFB microburst was a very wet one. It produced 0.71" of rainfall at the Base Weather Station, approximately 1 mile south of the microburst center. The wettest microburst in JAWS produced 0.24" in 4 minutes, a 3.6" per hour rate. In NIMROD, the wettest one was 0.58" in 4 minutes or 8.7" per hour. In a very wet microburst, an aircraft may disappear in heavy rain during its climbout phase.

Q: Is dry microburst generally weaker than wet microburst?

A: No, this is not always the case. The strongest JAWS microburst, with 57 mph wind, was a dry microburst. An innocuous shower or a virga in the Denver area could induce 40 to 60 mph winds.

"About the author"

TETSUYA THEODORE FUJITA

Born on October 23, 1920 at Kitakyushu City, Japan

- ■ 1953 D. Sc. from Tokyo University, Tokyo, Japan
- ■ 1953 Research Associate, Department of Meteorology, University of Chicago
- ■ 1956 Director, Mesometeorology Research Project, University of Chicago
- ■ 1962 Associate Professor, Dept. of Geophysical Sciences, Univ. of Chicago
- ■ 1965 Professor, Department of Geophysical Sciences, University of Chicago
- ■ 1968 Became a U.S. Citizen

Wind-shear related Awards

- ▲1977 Admiral Luis de Flores Flight Safety Award, Flight Safety Foundation
- ▲1977 Distinguished Service Award, Flight Safety Foundation
- ▲1979 Distinguished Public Service Medal, NASA
- ▲1982 Losey Atmospheric Sciences Award, AIAA

Wind-shear related Publications

- ● 1976 Spearhead echo and downburst near the approach end of a John F. Kennedy Airport runway, New York City. SMRP Res. Paper 137, University of Chicago, 51 pp.
- ● 1977 Spearhead echo and downbursts in the crash of airliner. Monthly Weather Review, 105, 129-146. (Fujita and Byers)
- ● 1977 Analysis of three weather-related aircraft accidents. Bulletin of American Meteorological Society, 58, 1164-1181. (Fujita and Caracena)
- ● 1977 Common denominator of three weather-related aircraft accidents. Preprint, 10th Conf. on Severe Local Storms, Omaha, 135-142. (Fujita and Caracena)
- ● 1978 Wind shear at Dulles Airport on 18 May 1977. SMRP Res. Paper 159, University of Chicago, 19 pp.
- ● 1980 Downbursts and microbursts - An aviation hazard. Preprints, 19th Conf. on Radar Meteorology, Miami Beach, Fla., 94-101.
- ● 1981 Microburst as an aviation wind-shear hazard. Preprint, 19th Aerospace Science Meeting, St. Louis, AIAA-81-0386, 9 pp.
- ● 1981 Five scales of airflow associated with a series of downbursts on 16 July 1980. Monthly Weather Review, 109, 1438-1456. (Fujita and Wakimoto)
- ● 1981 Tornadoes and downbursts in the context of generalized planetary scale. Journal of Atmospheric Sciences, 38, 1512-1534.
- ● 1982 Effects of miso- and mesoscale obstructions on PAM winds obtained during the Project NIMROD. Journal of Applied Meteorology, 21, 840-858.
- ● 1983 Microburst wind shear at New Orleans International Airport, Kenner, Louisiana on July 9, 1982. SMRP Res. Paper 199, University of Chicago, 39 pp.
- ● 1983 Microburst in JAWS depicted by Doppler radars, PAM, and aerial photographs. Preprints, 21st Conf. on Radar Meteorology, Edmonton, Canada, 638-645. (Fujita and Wakimoto)
- ● 1983 JAWS microbursts revealed by triple-Doppler radar, aircraft and PAM data. Preprints, 13th Conf. on Severe Local Storms, Tulsa, 97-100. (Fujita and Wakimoto)
- ● 1983 Analysis of storm-cell hazards to aviation as related to terminal Doppler radar siting and update rate. SMRP Res. Paper 204, University of Chicago, 90 pp.